





Article

Some Observations on Phytoplankton Community Structure, Dynamics and Their Relationship to Water Quality in Five Santiago Island Reservoirs, Cape Verde

Manuela Morais ^{1,2,*}, Alexandra Marchã Penha ^{1,2}, Maria Helena Novais ^{1,2}, Leonel Landim ³,
Sónia Silva Victória ³, Eduardo A. Morales ^{1,2} and Luciana Gomes Barbosa ⁴

- ¹ Institute of Earth Sciences—ICT, University of Évora, Rua Romão Ramalho 59, 7000-671 Évora, Portugal; mapenha@uevora.pt (A.M.P.); hnovais@uevora.pt (M.H.N.); edu_mora123@outlook.com (E.A.M.)
² Water Laboratory, University of Évora, P.I.T.E. Rua da Barba Rala No. 1, 7005-345 Évora, Portugal
³ Faculty of Science and Technology, University of Cape Verde, Praia 279, Cape Verde; leonel.landim@gmail.com (L.L.); sonia.silva@docente.unicv.edu.cv (S.S.V.)
⁴ Department of Phytotechny and Environmental Sciences, Federal University of Paraíba, Areia 58397 000, Brazil; lgomesbarbosa@gmail.com
* Correspondence: mmorais@uevora.pt; Tel.: +351-266740800

Abstract: Reservoirs provide valuable services to human beings, especially in arid, semi-arid, and Mediterranean regions affected by water scarcity. The present effort aims to study the environmental descriptors of variation and the main factors influencing phytoplankton composition, structure, and diversity in five reservoirs in Santiago Island, Cape Verde, a region affected by water availability. Five campaigns took place from 2016 to 2020 to sample phytoplankton and measure environmental variables according to standard analytical methodologies. Environmental results (17 water physico-chemical variables, air temperature, and precipitation) revealed that reservoirs differ in the geological influence variables. The high levels of P and N in water seem to be related to Land Use/Land Cover and are responsible for water-quality degradation. Cyanobacteria dominated the phytoplankton community and posed high risk levels, especially considering that the identified taxa are potential producers of different toxins. Taxa responsible for this dominance were not the same in all reservoirs, emphasizing the dominant role of local habitat factors on community composition and diversity. Overall, the results reveal the importance of defining integrated management plans/strategies for the set of five studied reservoirs, since the processes influencing variation in the phytoplankton community are temporal-scale dependent, with similar biogeographic patterns.

Keywords: cyanobacteria; cyanotoxins; diversity; eutrophication; public health; risk assessment; semi-arid climate



Citation: Morais, M.; Penha, A.M.; Novais, M.H.; Landim, L.; Victória, S.S.; Morales, E.A.; Barbosa, L.G. Some Observations on Phytoplankton Community Structure, Dynamics and Their Relationship to Water Quality in Five Santiago Island Reservoirs, Cape Verde. *Water* **2021**, *13*, 2888. <https://doi.org/10.3390/w13202888>

Academic Editor: George Arhonditsis

Received: 1 September 2021

Accepted: 11 October 2021

Published: 15 October 2021

Publisher's Note: MDPI stays neutral with regard to jurisdictional claims in published maps and institutional affiliations.



Copyright: © 2021 by the authors. Licensee MDPI, Basel, Switzerland. This article is an open access article distributed under the terms and conditions of the Creative Commons Attribution (CC BY) license (<https://creativecommons.org/licenses/by/4.0/>).

1. Introduction

Dams have been used as important strategies to face water scarcity in regions where this resource needs to be stored for human development. In this situation, arid, semi-arid, and Mediterranean regions stand out since reservoirs have provided valuable services such as drinking water supplies, hydropower, and irrigation [1–4].

Phytoplankton plays an important role in maintaining the balance of reservoirs by consuming carbon dioxide and nutrients and releasing oxygen. The structure of this community is closely related to environmental factors, particularly nutrients, water temperature, and light availability [5–7]. Increasing water temperature gives Cyanobacteria a selective advantage over other phytoplankton groups. Therefore, monitoring and forecasting of the phytoplankton community are of great importance, especially when changes are driven by human activities, such as agriculture, livestock, wastewater, and urban runoff. In this context, phytoplankton can act as an alert proxy, indicating eutrophication levels and undesirable changes in the ecosystem. One of the best-known changes associated with

eutrophication is the mass development of Cyanobacteria, which occur worldwide in many lakes, reservoirs, and rivers [8–10]. Dense accumulations of Cyanobacteria are commonly associated with nutrient-rich, warm ecosystems with little movement or mixing among layers [11].

Cyanobacteria are often potentially toxin-producing organisms and can compromise the use of water by putting human and animal health at risk [12–14]. These situations are a major concern for entities responsible for water treatment, supply systems, and health-related institutions. Additionally, some authors predict that the proliferation of toxic Cyanobacteria will occur more frequently in the future because of global warming and climate change [15–19]. Studies suggest that toxic *Microcystis* genotypes are favored over non-toxic ones at warmer temperatures [20]. Among the most prevalent cyanotoxins is Microcystin, which can be detected in planktonic genera but also in benthic Cyanobacteria [21]. In freshwater ecosystems, the most abundant and spread out Microcystin-producing genera are *Microcystis*, *Planktothrix*, and *Dolichospermum* [22]. Those genera are largely distributed in eutrophic waters enriched with P and N and can move along the water column of turbid and shallow water systems to uptake resuspended P from sediments [21]. Microcystins, which are encoded by the *mcy* cluster (microcystin synthetase), have been categorized in several cyanobacterial genera [23,24]. This cluster contains nine to ten genes, and the detection of genes from the *mcy* cluster usually indicates the presence of potentially toxic Cyanobacteria [21]. Concerning Nodularins, these are encoded by the *ndaS* gene cluster, and the projected biosynthetic pathway shares a similar structure with the *mcy* gene cluster [25]. Blooms of Nodularin-producing species, namely *Nodularia spumigena*, are mainly present during late summer, in N-reduction conditions with a low N:P ratio and high temperatures, where other phytoplanktonic species cannot grow [25,26].

In shallow eutrophic waters, particularly in tropical latitudes, Cyanobacteria are more frequent, where key drivers are the constant light and temperature conditions [27]. In these conditions, blooms persist year-round [28–30]. Droughts also play an important role in cyanobacterial bloom dynamics [31–34]. The absence of precipitation during drought events reduces water availability and affects multiple ecological conditions [35,36]. In fact, droughts have been reported to favor cyanobacterial dominance [32–37]. Contrariwise, extreme prolonged drought in shallow lakes may also limit Cyanobacteria due to high inorganic turbidity, in favor of mixotrophic organisms or diatoms [33,38].

The complexity of these dynamics is higher in arid environments because of the wide hydrological fluctuations brought by long-lasting droughts, combined with the high unpredictability of rainfall events, which has been aggravated due to climate change [39]. Semi-arid regions may be the most sensitive areas to global changes because of their fragile ecosystems [40]. In these regions, potential evaporation exceeds precipitation on an annual average basis, and landscapes are characterized by dry climates, low vegetation cover, high erosion, and low water infiltration capacity of the soil [40]. Therefore, understanding the environmental patterns and the drivers that regulate the structure of biological communities in reservoirs located in semi-arid regions is pivotal for the implementation of an integrated management strategy that prevents anthropogenic degradation and, consequently, consolidates ecosystem conservation, as well as human and animal health.

In Cape Verde, the problems related to water scarcity arise in a particular way. The archipelago is located 450 km from Senegal, comprising a vast region of arid and semi-arid climate that also covers the entire northwest of the African Continent, in transition to the desert climate. Until very recently, the water exploited in Santiago Island was mostly of underground origin, coming from springs, wells, and boreholes in an estimated total of 53,989 m³ per day, with springs contributing about 44%, boreholes 28%, and wells 29% [41]. The use of underground resources was close to the maximum, which imposed an urgent mobilization of means to allow the use of water from other sources, especially for agriculture activities [41]. Therefore, in 2006, the first dam was built in Cape Verde, and others soon followed, making a total of nine dams, seven of which were built on Santiago Island. The objectives of this governmental option were to increase the access to

water for the irrigation of agricultural land, and the storage capacity to cope with drought periods [42].

Regarding the study of these reservoirs, there are some data on their characteristics, mostly academic studies that refer to particular aspects of the reservoirs, especially the oldest one, Poilão [42–46]. However, there are no comparative studies on water quality and ecological integrity that could be used to support the implementation of integrated basin management to protect these sensitive systems that are extremely vulnerable to accelerated degradation that puts public health, and ultimately water use, at risk.

In this framework, the present study aims to investigate environmental descriptors of variation and the main influencing factors on phytoplankton taxonomic composition, structure, and diversity, including cyanobacterial dominance and toxin production in five reservoirs in Santiago Island.

We tested the following hypotheses:

1. The variation in phytoplankton taxonomic composition within each reservoir is mainly governed by local environmental conditions due to the high dispersal ability of phytoplankton at small spatial scales (Santiago Island scale).
2. Phytoplankton abundance, community composition, and cyanobacterial dominance are dependent on the quantity of the water and nutrient inputs in the reservoirs.

It is expected that the obtained results will be useful to promote the protection of these strategic water reserves and highlight the need to implement Hydrographic Basin Plans in Cape Verde, promoting ecological integrity and environmental health.

2. Materials and Methods

2.1. Study Area: Regional Context

The Cape Verde archipelago is located on the eastern edge of the North Atlantic, about 450 km of the west coast of Africa, 1400 km South-southwest (SSW) of the Canary Islands, limited by parallels 17°13' and 14°48' of north latitude and through meridians 22°42' and 25°22' of west longitude. The archipelago is formed by ten islands, nine of which are inhabited, and thirteen islets, which occupy a total area of 4033 km² and an exclusive economic zone (EEZ) that extends over approximately 700,000 km² (Figure 1). According to data from the National Institute of Statistics (INE), Continuous Multi-Objective Survey, Body Mass Index (BMI) [47], the Cape Verde archipelago has a resident population of 549,699 inhabitants. The archipelago has a maximum elevation of 2829 m a.s.l. on Fogo Island; geologically, it is made up of sub-aerial, predominantly basaltic, emissions from lava flows and pyroclastic materials (i.e., slag, bagacin, or lapilli and ash) [48]. Therefore, soils are generally coarse textured and thin, with reduced ability to retain water. Globally, Cape Verde has an average temperature of 25 °C, presenting, like other Sahelian countries, two seasons: A dry season, from December to June, and a wet season, from August to October. July and November are considered transitional months. According to [49], more than 75% of the average annual precipitation, around 300 mm, occurs in August and September. However, the Cape Verde archipelago presents islands with a predominantly arid climate and others with a predominantly semi-arid climate. The rainy season has an average duration of 15 to 25 days in the arid areas, and 45 to 55 days in the semi-arid areas.

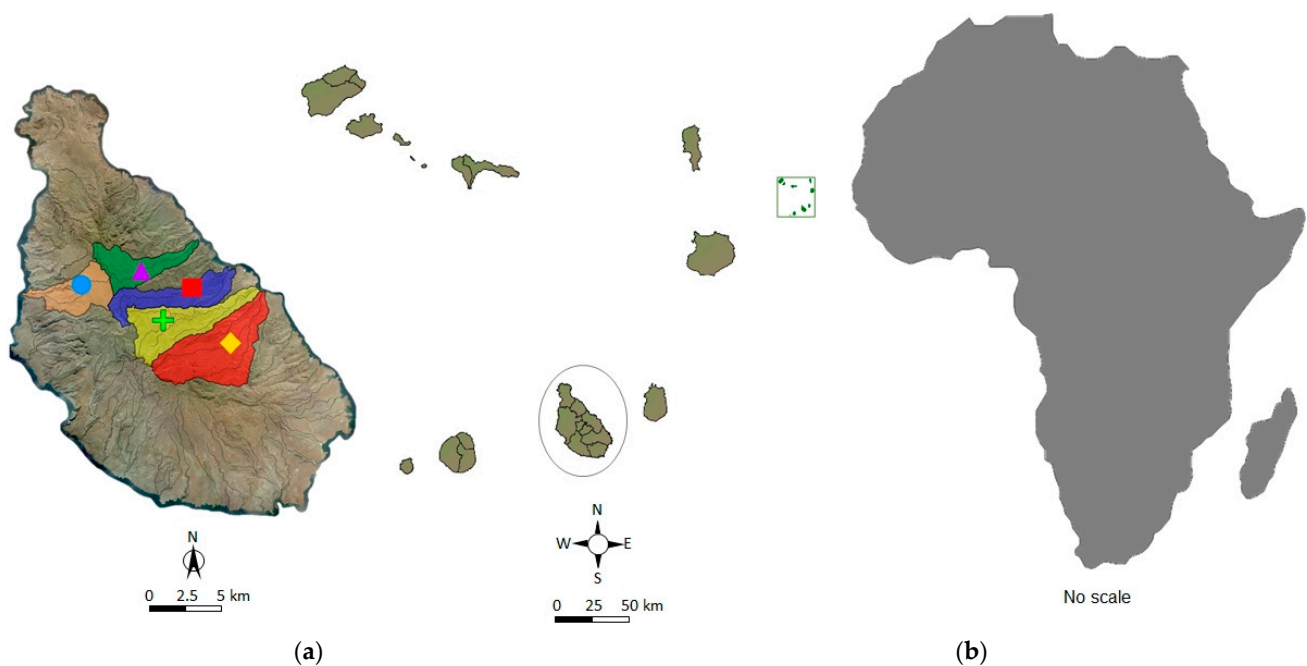


Figure 1. (a) Santiago island with the five drainage basins of the main rivers, where the studied reservoirs are located. ● Saquinho reservoir; ▲ Flamengos reservoir; ■ Figueira Gorda reservoir; + Faveta reservoir; ◆ Poilão reservoir. (b) Map of Cape Verde archipelago showing its location on the west coast of Africa with Santiago Island identified within a circle. The map of Africa is not to scale.

Santiago Island is in the southern part of the Cape Verde archipelago, between the parallels $15^{\circ}20'$ and $14^{\circ}50'$ of north latitude and the meridians $23^{\circ}50'$ and $23^{\circ}20'$ of west longitude (Figure 1b). It is the largest of the ten inhabited Cape Verde islands, with an area of 991 km^2 , corresponding to about 25% of the total archipelago area. Santiago Island is elongated in the NNW-SSE direction and presents rugged relief with wide and open valleys. The highest point is Pico de Antónia at 1394 m a.s.l., located in the south-central part of the island. The northern two-thirds of the island is cut by deep valleys, but in certain places (i.e., west of the city of Assomada and the center of the island) there are sloping paleotopographies that can be recognized as comprising large non-conformities covered by younger lavas [50]. Regarding data from [47], the island has an estimated population of 309,372 inhabitants, administratively distributed in nine Municipalities (Tarrafal, Santa Catarina, Santa Cruz, Praia, S. Domingos, S. Miguel, S. Salvador do Mundo, S. Lourenço dos Órgãos, and Ribeira Grande de Santiago). The rainfall follows the characteristic archipelago seasonality (an annual mean of around 300 mm), with the wet period between August and October. According to [51], the relief and far southern location of the island contribute to greater precipitation compared to other islands, and the steep slope mainly leads the superficial water flows towards the sea. Regarding vegetation (ranging from cactus at low altitudes to pampas, steppes, and grassland vegetation at higher altitudes), the Santiago Island vegetation is intrinsically linked to climatic conditions and human settlements. Thus, the current vegetation consists largely of species introduced by man and other vectors such as birds and marine currents [52]. In this context, [53] notes the importance of deliberate uses, but with a lack of control, of certain exotic species in reforestation and soil conservation actions in Cape Verde, namely *Prosopis juliflora* (Sw.) DC., *Leucaena leucocephala* (Lam.) de Wit, and *Furcraea foetida* (L.) Haw., which has translated into invasions of native vegetation habitats. In the case of the American Acacia (*Prosopis juliflora*), [53] showed that currently this species is distributed throughout the archipelago (except for São Nicolau), having been extensively planted due to its resistance to dry conditions [54].

Water scarcity and the geomorphological characteristics promoted investment from the governments of Cape Verde in the construction of infrastructure (dams), aiming to increase the availability of water for agriculture (Table 1). The first to be built was the Poilão

dam, followed by the construction of six more on Santiago Island (Table 1). From these, in the framework of this study, Poilão, Saquinho, Faveta, Figueira Gorda, and Flamengos were assessed, but Salineiro and Principal dams had to be excluded because the first one retains little water due to infiltration problems and the construction of the second was not completed by the time this study was finished.

Table 1. Characteristics of the dams on Santiago Island, Cape Verde, including depth in each of the sampling periods. Dam characteristics recorded from [55].

	Poilão	Saquinho	Salineiro +	Faveta	Figueira Gorda	Flamengos	Principal +
Stream	Ribeira Seca	Ribeira Charco	Ribeira Grande	Ribeira Picos	Ribeira Boaventura	Ribeira Flamengos	Ribeira Principal
Year of construction	2006	2013	2013	2013	2014	2017	2019
Maximum height (m)	26.0	33.9	31.0	36.5	34.7	32.5	42.8
Maximum capacity (10 ³ m ³)	1700	700	700	700	1800	850	700
Available water volume for irrigation (10 ³ m ³ /year)	1200	563	596	536	1455	852	520
Irrigated area (ha)	100	66	58	86	105	80	85
Maximum flood discharge (m ³ /s)	320.0	312.0	214.5	186.6	363.0	271.0	200.0
Reservoir depth in June 2016 (m)	8	*	*	10	8	9	*
Reservoir depth in May 2017 (m)	7	*	*	9	8	7	*
Reservoir depth in December 2017 (m)	4	6	*	9	8	7	*
Reservoir depth in October 2018 (m)	4	5	*	*	9	*	*
Reservoir depth in February 2020 (m)	*	1	*	*	4	1 **	*

+ not included in the present study; * not sampled; ** depth of the remaining pools inside the reservoir.

Considering the possible human influence on reservoir water characteristics, as well as local populations' access to water and sanitation, these data were also consulted and are summarized in Table 2. The information includes data for the year 2019 on the number of inhabitants of Cape Verde and of the municipalities where the reservoirs are located, as well as data on the access to water, solid waste evacuation, and wastewater evacuation [47], differentiated by a water network connected or not connected to the public, as well as means of evacuation.

Table 2. Water access, sanitation (wastewater and solid waste evacuation), and inhabitants of Cape Verde, and municipalities most represented in each of the drainage basins on which reservoirs are located in Santiago Island. Data of water access and sanitation are in percentage (%); inhabitant data are in absolute number (N°). Flamengos reservoir is located in the municipality of S. Miguel, Saquinho reservoir in Santa Catarina, Figueira Gorda reservoir in S. Cruz, Faveta reservoir in S. Salvador do Mundo, and Poilão reservoir in S. Lourenço dos Orgãos.

Water Access and Sanitation		Cabo Verde	Urban Area	Rural Area	São Miguel	Santa Cruz	Santa Catarina	São Lourenço dos Orgãos	São Salvador do Mundo
Access to Water	Connected to the network	69.0	74.7	57.4	52.2	69.0	57.7	56.2	15.6
	Not connected to the network	31.0	25.3	42.6	47.6	31.0	42.3	43.8	84.4
	Neighbours	9.3	11.9	3.9	4.3	7.8	4.2	4.2	0.0
	Engine	8.5	7.8	10.0	4.4	5.2	14.8	12.5	26.3
	Fountain	7.1	5.0	11.7	8.8	4.9	6.5	1.9	16.3
Other sources	6.1	0.5	17.2	30.3	13.1	16.8	25.2	41.8	

Table 2. Cont.

Water Access and Sanitation		Cabo Verde	Urban Area	Rural Area	São Miguel	Santa Cruz	Santa Catarina	São Lourenço dos Órgãos	São Salvador do Mundo
Wastewater evacuation	Connected to the sewer network	31.6	44	3.3	54.9	29.6	3.8	1.0	1.1
	Septic tanks	51.0	43.4	68.4	6.2	22.4	69.0	74.7	71.9
	Rudimentary septic tanks	2.6	2.5	2.7	0.0	10.3	2.6	0.0	0.0
	No access-discharge into the nature	14.8	10.1	25.6	38.9	37.7	24.6	24.3	27.0
Solid waste evacuation	Connected to the management system								
	Containers	59.1	65.2	46.6	49.4	56.9	35.1	57.0	52.4
	Dump trucks	23.0	31.5	5.6	3.2	1.5	2.9	1.1	4.5
	No connection to the management system								
	Buried/Burned Dumped into the nature/surroundings of the houses	9.6	1.6	26.7	20.8	15.0	39.3	33.0	23.0
		8.3	1.7	21.1	26.5	16.7	22.7	8.9	20.1
Inhabitants		549,699			13,779	25,917	47,604	6,879	8,582

Table 2 shows that 31.0% of the Cape Verde population does not have access to piped water from the public network, especially in rural areas where this percentage reaches 42.6% of the population, with higher values for S. Miguel, S. Lourenço dos Orgãos, and especially in São Salvador do Mundo municipalities, where 84.4% of the population is not connected to the public network. Under these conditions, the population is mostly supplied by auto-tanks, public fountains, and other sources, such as boreholes, wells, and springs. Furthermore, 68.4% of the Cape Verdean population does not have a connection to the public sewer network for the evacuation of wastewater. In rural areas, the situation is more serious, with 96.7% of the population not having this connection, using rudimentary septic tanks and nature for their discharges. This situation is particularly dramatic in the municipalities of Santa Catarina, S. Lourenço dos Orgãos, and São Salvador do Mundo, with only 3.8%, 1.0%, and 1.1% of the population connected to the public sewer network. In these municipalities, septic tanks represent the main means of evacuation. However, it should be noted that the discharge directly into nature is extremely high, above 25% in rural areas, particularly in the municipalities where the five reservoirs are located. Concerning solid waste, evacuation systems include junk cars and containers, the latter being one of the main types of discharge connected to the public system (65.2% in urban areas, 46.6% in rural areas). However, the percentage of the population that is not connected to the evacuation system is very high, especially in rural areas, with emphasis on the municipalities of S. Miguel (47.3%), Santa Cruz (31.7%), Santa Catarina (62%), S. Lourenço dos Orgãos (41.9%), and S. Salvador do Mundo (43.1%). It should also be noted that in these municipalities, the percentage of solid waste that is dumped into nature/surroundings from households is high (higher than 20% in the municipalities of S. Miguel, Santa Catarina, and S. Salvador do Mundo).

2.2. Geological Units and Land Use/Land Cover Characterization of Reservoir Drainage Basins

To characterize the geological units for the five drainage basins (Figure 1a), an analysis of spatial data was carried out using the Geographic Information System (GIS), ArcGIS Software version 10.7.1 (Coordinate System: Lambert Conformal Conic 2SP; Projection: Lambert Conformal Conic; Datum: WGS 1984). Subsequently, a map of the geological units of the hydrographic basins (Figure 2) was prepared based on the Geological Map of Santiago Island at a scale of 1:100,000 [56], with the basin limits calculated through the IDECV website [51].

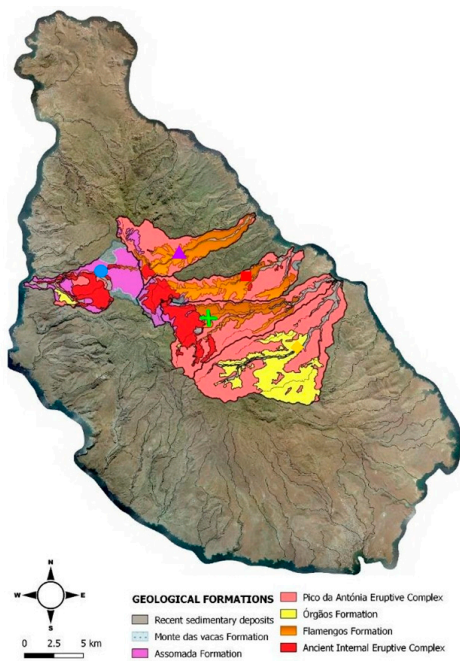


Figure 2. Map of geological units of the five drainage basins with the dam location on the main river. From North to South: Flamengos in Flamengos stream ▲; Saquinho in Charco stream ◆; Figueira Gorda in Boaventura stream ■; Faveta in Picos stream +; Poilão in Seca stream ◆.

Similarly, the percentage of Land Use/Land Cover (LULC) in each drain basin (Figure 3) was estimated by Remote Sensing (DR) and by GIS techniques. First, the website <https://earthexplorer.usgs.gov/> (accessed on 29 April 2019) was used to obtain the satellite images. Then, the classification of images was conducted by analyzing the cartographic database (MDT) at the National Institute of Territory Management [57]. The classification of Landsat 5 images and the respective validation was performed using GIS modelling (ArcGIS 10.6) software, obtaining the LULC per pixel, referring to the previously defined occupation and land use classes using the maximum likelihood classification tool: Agriculture, vegetation, urban settlements, erosion area, bare soil, and agroforestry. It is noteworthy that the LULC estimation was conducted for 2018, which serves as a reference for the study period (2016–2020).

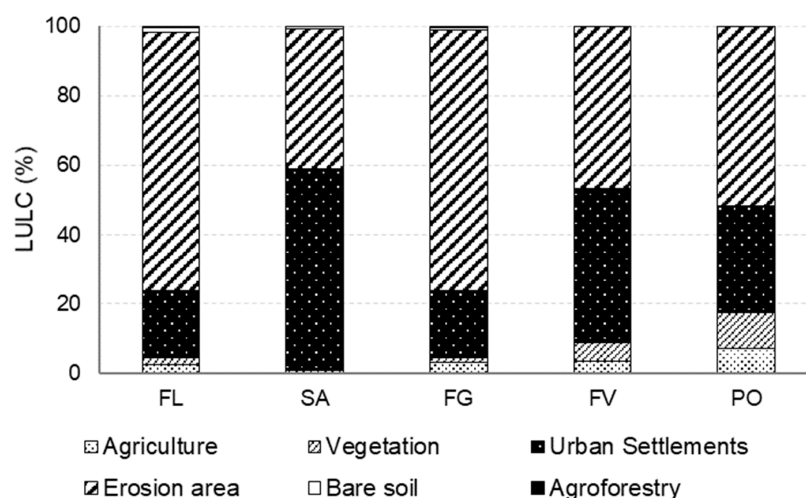


Figure 3. Percentage of the LULC classes in the selected drainage basins. FL—Flamengos basin. SA—Charco basin. FG—Boaventura basin. FV—Picos basin. PO—Seca basin.

2.3. Meteorological Characterization

The meteorological data of air temperature and monthly accumulated precipitation during the study period were obtained from the five closest meteorological stations to the reservoirs, operated by the National Institute of Meteorology and Geophysics (Figure 4). Additionally, to characterize the extension of the dry period during the study period, a thermo–pluviometric diagram was prepared using the GAUSSEN method (Figure 5). This method considers dry months as those in which $PPT < 2 T$ (PPT represents the monthly accumulated precipitation in mm and T the monthly mean air temperature in °C).

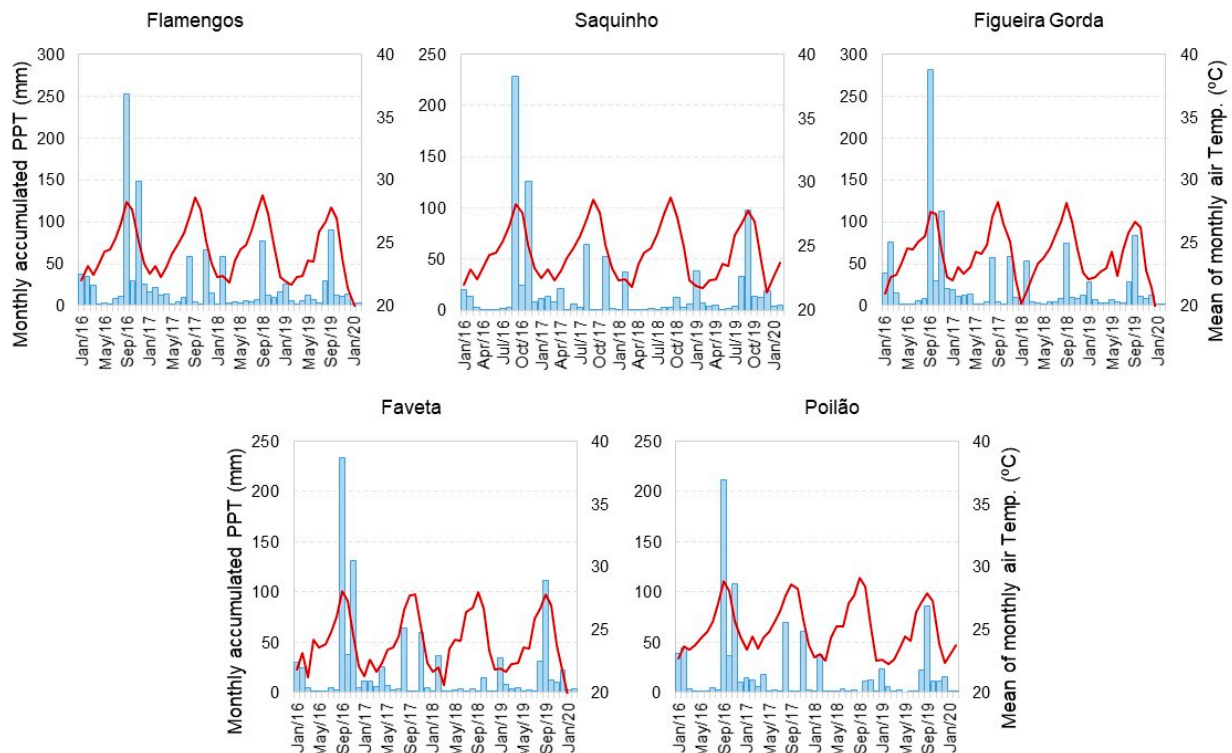


Figure 4. Precipitation and temperature graphs from the meteorological stations that better characterize each reservoir. Monthly mean air temperature (red line); monthly accumulated precipitation (blue bars).

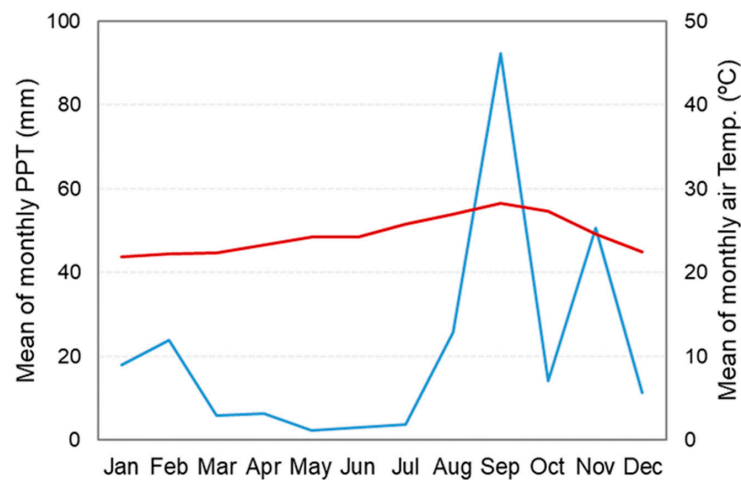


Figure 5. Extension of the dry period (2016–2020). Mean of monthly accumulated precipitation (blue line) and temperature (red line) data obtained from the five meteorological stations that better characterize each reservoir.

2.4. Sampling Sites and Periods

The reservoirs of Poilão, Faveta, Figueira Gorda, Saquinho, and Flamengos on Santiago Island (Figures 1a and 2) were sampled from 2016 to 2020 episodically in five campaigns: June 2016, May 2017, December 2017, October 2018, and February 2020. These campaigns took place mostly in the dry season, except for October 2018, which theoretically belongs to the wet season. In fact, 2017, 2018, and 2019 correspond to three years of drought, with annual rainfall well below the average for the country.

It should be noted that (i) sampling in Flamengos only started in December 2017, at the beginning of the filling, after the completion of the dam construction; (ii) in October 2018, only Flamengos, Figueira Gorda, and Poilão were sampled, since Saquinho and Faveta were dry; (iii) for the same reason, in 2019, no sampling campaign was carried out; and (iv) since the drought in Cape Verde was extended, in February 2020, Figueira Gorda and Flamengos were sampled, with the latter only in two persistent pools (pool 1: ~30 m², also called “big pool”; and pool 2: ~15 m², named “small pool”), fed by groundwater.

2.5. Environmental Parameters

In each campaign, in the deepest point closest to the dam of each reservoir, an in situ water physical-chemical characterization was carried out using a TROLL 9500 PROFILER XP multi parametric probe to measure temperature (T, °C), pH, dissolved oxygen (DO, % of O₂ saturation), and depth (m). Simultaneously, water samples were collected at two depths (surface and bottom), using a Van Dorn bottle (capacity of 3 L). These samples were refrigerated (at 4 °C) until transport (no longer than 3 days) in polyethylene containers to the Water Laboratory, University of Évora, Portugal for laboratory analysis. The reservoirs depth in each of the sampling periods, as an indicator of the availability of water in each of the systems, is presented in Table 1. The chemical parameters were analyzed according to standard methods [58]: Total nitrogen (TN, mg N/L), nitrates (NO₃, mg N/L), ammonium (NH₄, mg N/L), total phosphorus (TP, mg P/L), sodium (Na, mg/L), potassium (K, mg/L), calcium (Ca, mg/L), chlorides (Cl, mg/L), sulfates (SO₄, mg/L), carbonates (CO₃, mg/L), bicarbonates (HCO₃, mg/L), magnesium (Mg, mg/L), and silica (SiO₂ mg Si/L). Additionally, the N:P ratio was computed, with the TN and TP analyzed.

2.6. Phytoplankton

2.6.1. Phytoplankton Assemblages and Diversity

For phytoplankton analysis, at each site, a composite sample representative of the euphotic zone (calculated as 3.0 times the Secchi disk depth [59]) was conducted, using a Van Dorn bottle (capacity of 3 L) [60]. Phytoplankton samples were immediately preserved in the field with Alkaline Lugol’s solution (0.5%).

In the laboratory, phytoplankton was identified to the lowest taxonomical level using an inverted microscope (Leica DMIL, 1000× magnification) and specific bibliography [61–68]. Phytoplankton quantification was carried out with an inverted microscope using sedimentation chambers of different volumes [69]. The phytoplankton biovolume was estimated on the basis of geometrical formulas [70,71] using an average of 20–30 individuals and was expressed in mm³/L [72]. Two complementary matrices were obtained at the end of the identification process: Density and biovolume matrix.

An analysis of diversity was carried out following metrics and indexes calculated using Paleontological Statistics software (PAST v.4.03) [73]: (i) The Shannon Index (H′) [74] measures the degree of uncertainty in predicting to which taxon an individual randomly removed from the population would belong; (ii) Margalef’s diversity index (M) is a richness index that compensates the effects of sample size by dividing the number of taxa into a sample by the natural log of the number of individuals [75]; (iii) the Evenness index [76] refers to the similarity of frequencies of the taxa in a population; and (iv) the dominance index (1–Simpson’s Index) varies from 0 (with all taxa present in equal amounts) to 1. Sequentially, the total number of taxa of each sample was evaluated through the alpha diversity (α), i.e., taxa richness.

In order to evaluate how α diversity varies along the temporal gradient of the study period, and to follow the renewal or replacement of taxa over the study period, the beta diversity (β) was determined through the utilization of two different indexes. The first is a dissimilarity index of $\beta - 1$ [77], which measures how much regional diversity exceeds the average α diversity, calculated by the expression $\beta - 1 = \frac{\left(\frac{S}{\alpha_{\text{medium}}}\right)^{-1}}{N-1}$, where S is the regional diversity (gamma diversity [γ], number of taxa in the group of reservoirs in each period), α_{medium} is the average α diversity for the group of reservoirs in each period, and N is the number of reservoirs in the period. The second is a similarity index (Sorensen index), which measures how much the average similarity exceeds the γ diversity, calculated by the expression $\beta = \frac{2 \times C}{\sum_i S_i}$ where C corresponds to the number of common taxa and S is the regional diversity.

2.6.2. Risk Levels of Toxic Cyanobacteria Occurrence

The global and individual reservoir risk levels for each sampling period were determined according to the WHO Guidelines in Bathing Waters [78], using the Cyanobacteria cell density criterion, based on four different classes: (i) No Risk (no detection of Cyanobacteria), (ii) Low Risk (Cyanobacteria density <20,000 cells/mL), (iii) Moderate Risk (Cyanobacteria density between 20,000 cells/mL–100,000 cells/mL), and (iv) High Risk (Cyanobacteria density >100,000 cells/mL). Despite the fact that this criterion was specifically proposed for bathing waters, it constitutes a good indicator for the assessment of potential risk for animals and human exposure/contact.

To complement the risk level assessment, and due to the constant frequency of high densities of Cyanobacteria in the studied reservoirs, the presence of potentially toxin-producing Cyanobacteria and toxin-producing genes of microcystins, nodularins, and cyndrospermopsin were tested and identified using molecular biology techniques for the two last campaigns (October 2018 in Flamengos, Figueira Gorda, and Poilão reservoirs, and February 2020 in Flamengos and Figueira Gorda reservoirs).

These molecular biology techniques, such as the Real-Time Polymerase Chain Reaction (RT-PCR), were carried out after total DNA extraction using TRIidty GTM according to manufacturer indications. For the RT-PCR reaction, each well contained 1 × iTaqTM universal SYBR[®] Green Supermix (Bio-Rad, Hercules, CA, USA), 250 nM of each primer sequence, 0.5 μM Bovine Serum Albumin (BSA), and 1 μL of template DNA, in a total of 20 μL per well. Duplicates of all samples were prepared. The Real-Time PCR procedure started with the first denaturation step at 95 °C for 5 min, followed by the second step with denaturation at 95 °C for 10 s, annealing at 58 °C for 20 s, and an elongation step at 72 °C for 30 s. This second step was repeated for 40 cycles. As the final step for the melting temperature determination, the temperature started at 65 °C and increased every 0.5 s until it reached 95 °C. The results were expressed considering the melting curves for each gene, since for each PCR product, there is a specific melting curve. Therefore, each time the denaturation peak surpasses the baseline, the result is considered positive, that is, there is the presence of the specific target gene in the respective sample [79]. The genes, amplicon size with respective melting peaks temperatures, references, and what the sequences represent for each gene are represented in Table 3. The results are represented as melting curve graphs using Bio-Rad CFX Manager software (Bio-Rad, Hercules, CA, USA).

2.7. Statistical Analysis

2.7.1. Environmental Parameters

The statistical analysis of the environmental parameters was based on a matrix of 17 variables × 32 samples. A multivariate ordination analysis was carried out to analyze the entire dataset. The ordination was made through a principal component analysis (PCA), using the software Paleontological Statistics (PAST v. 4.03) [73]. Data were previously transformed by $\log(x + 1)$, not only to bring the data closer to normality, but also to improve the recovery power of patterns and minimize the influence of the variances of each variable

and of the various measurement units [85]. Prior to further data processing, a normality analysis was carried out (Shapiro–Wilk W).

Table 3. Primer sequences for specific target genes with respective amplicon size (base pairs, bp), specific melting temperature, references, and observations.

Target Gene	Primer Direction 5'–3' (Forward and Reverse)	Amplicon (bp)	Melting Temp. (°C)	Reference	Observations
16S rRNA	AGAGTTTGATCCTGGCTCAG GCTTCGGCACGGCTCGGTCGATA	780	83.5–85.0 °C	[80,81]	Universal gene for identifying the presence of Cyanobacteria
<i>mcyB</i>	TGGGAAGATGTTCTTCAGGTATCCAA AGAGTGGAAACAATATGATAAGCTAC	350	78.0–79.5 °C	[82]	Genes specific for B and E regions of the Microcystin gene and common region of Microcystin and Nodularin gene-specific
<i>mcyE/nda</i>	TTTGGGGTAACTTTTTGGCCATAGTC AATTCTTGAGGCTGTAAATCGGGTTT	472	80.0–83.0 °C	[83]	
Peptide synthetase	GGCAAATTGTGATAGCCACGAGC GATGGAACATCGCTCACTGGTG	597	83.0 °C	[84]	Specific genes to produce proteins responsible for the synthesis of Cyindrospermopsin.
Polyketide synthetase	GAAGCTCTCTGGAATCCGGTAA AATCTTACGGGATCCGGTGC	650	81.0–82.0 °C	[84]	

After having verified that most data vectors did not follow a normal distribution, with p values lower than the comparison factor ($p = 0.05$), non-parametric tests were applied (Kruskal–Wallis and Pairwise Mann–Whitney) to analyze differences among reservoirs and sampling periods. In addition to the parameters that showed significant differences, line graphs were plotted.

Statistical analyses, specifically the normality (Shapiro–Wilk W , $p = 0.05$), non-parametric Kruskal–Wallis (significance factor $p < 0.05$), and Pairwise Mann–Whitney (significance factor $p < 0.05$) tests, were carried out using the Microsoft Excel supplemental software Real Statistics.

2.7.2. Phytoplankton

Regarding phytoplankton data, an exploratory analysis was carried out based on the density and biovolume of phytoplankton taxonomic groups for each reservoir by sampling period. As expected, the phytoplankton data did not follow a normal distribution, since the community presented different densities per species. In this sense, a non-parametric multidimensional scaling (nMDS) ordination was applied (Bray–Curtis distance, minimum stress 0.01, Kruskal fit scheme), based on the density of the phytoplankton matrix (92 taxa \times 19 samples). In addition, the differences between groups identified in the rankings were validated using a non-parametric similarity analysis (ANOSIM) [86]. This method uses the value of R to assess the difference between defined a priori groups, utilizing random permutations in the Bray–Curtis similarity matrix. In the next step, SIMPER analysis was applied to determine which species contribute the most to the differentiation of groups and which contribute to the similarity within each group [87]. nMDS, ANOSIM, and SIMPER analyses were performed using the PRIMER v. 5.2.0 program [87].

To evaluate the role of Cyanobacteria (density and biovolume) in shaping the phytoplankton community, non-parametric Spearman correlations were performed between this group and different diversity metrics/indexes: The Shannon Index (H'), Margalef's diversity index (M), Evenness index (J), Dominance index (D), α diversity, Density (N°), and Biovolume (Bv).

2.7.3. Relationship between Environmental Variables and Phytoplankton Descriptors

A multiple-regression analysis by the least-squares method and descending stepwise procedure was carried out to analyze the influence or relationship of the environmental variables in the phytoplankton structure (i.e., structural community metrics: Total density, Cyanobacteria density, Bacillariophyta density, Chlorophyta density, total biovolume, Cyanobacteria biovolume, Bacillariophyta biovolume, Chlorophyta biovolume, H' , M , J , D , and α diversity). In this analysis, Cryptophyta, Dinoflagellata, and Euglenophyta were discarded due to their low representation. The significance degree of the regressions

was tested by an analysis of variance, using the value of F for $p < 0.05$ as critical. The coefficient of determination (R^2) was calculated as a measure of the proportion of variance that is explained by the independent variables. Since the regression analyses assume the normality of the data, the data were transformed into $\log(x + 1)$ prior to the analysis. The multiple regression analysis was conducted using Paleontological Statistics software (PAST v.4.03).

3. Results

3.1. Geological Units and LULC Characterization

3.1.1. Characterization of Geological Units

In the drainage basins of the main rivers, where the dams are located, the geological units can be grouped from the oldest to the most recent in seven main complexes/formations [88,89] (Figure 2).

The Ancient Internal Eruptive Complex (CA) is present in the headwaters of the Ribeira de Boaventura and Ribeira de Picos basins and in the middle zone of the Ribeira do Charco basin following this stream to the mouth (Figure 2). This geological unit represents the substratum of the island, corresponding to the oldest formation that emerges due to the current level of erosion of the island, and constitutes the base of all other formations. It is characterized by the existence of a dense network of very altered lodes, being almost impossible to individualize in many of the spots.

The Flamengos Formation (FF) comprises the Flamengos, Boaventura, and Picos basins. It follows the Flamengos and Boaventura streams from the source to the mouth and a large part of the middle section of the Picos stream and its basin. This formation corresponds to a very extensive and uniform underwater volcanic sequence, consisting of mantles, breccias, and underwater pyroclasts, with great uniformity and extension. The Flamengos formation is exposed by erosion in deep valleys in the center of the island, and lavas dip 20° – 30° to the northeast.

The Pico da Antónia Eruptive Complex (PA) extends to the more southern basins (Ribeira Seca and Ribeira de Picos), occupying the northern part of the Flamengos basin and the areas furthest away from the Picos stream. Although it has little expression, it is also present in the Charco Basin in the central zone embedded in CA. The PA outcrops are responsible for the highest elevations and structural platforms on the island of Santiago. This complex includes pyroclastic products with explosive and effusive activities, and sub-air and sub-sea lavas. The lava mafic rocks of the PA are ultrabasic alkaline comprising basanites, melanephelinites, and nephelinites.

The Assomada Formation (AF) occupies the Charco stream basin, although its presence is residual in the headwater of Flamengos, Boaventura, and Picos basins. It is an eruptive formation made up of mantles, drainages, and basaltic pyroclasts, originating from an exclusively subaerial activity. The lavas constitute extensive, almost horizontal flows that reach the coast, having flowed to the west, creating an angular disagreement ($\sim 10^\circ$ – 12°) with the outflows of the PA.

The Monte das Vacas Formation (MV) is mainly present in the Ribeira do Charco basin, on the northern and southern borders of the upper part of the basin. It is also present in a small spot at the southern border of the Boaventura river basin (in the upper zone). This geological formation consists of a few dozen basaltic pyroclast cones (tufts, bagasse, bombs, and slag) and some small associated layers or drains. Originally the pyroclastic materials are black in color, but on the Island of Santiago, they have a reddish-brown color due to very advanced alteration.

The Recent Sedimentary Deposits (RC) follow the course of the main streams in each of the basins, especially in the downstream sections of the dams up to the mouth. The sedimentary formations (of the Quaternary age) constitute old alluviums in almost all the streams, currently forming terraces (gravel deposits) that are being progressively destroyed. There are also slope deposits, sometimes very thick and vast, as well as flood deposits and

recent river alluvium, forming floodplains that are sometimes very extensive. There are also sands and pebbles on the beach in the terminal section of the streams.

The Orgãos Formation (OF), in the Ribeira Seca basin, occupies the central area of the basin closest to the main river. It is also present in a small spot at the southern part of the Charco stream basin. This formation corresponds to a brechoid conglomerate formed by elements of various dimensions, and it marks a long period of relative calm in the eruptive activity and probably a humid climate favorable to intense water erosion.

3.1.2. LULC Characterization

The five drainage basins of the main rivers where the dams are located have similar LULC occupation patterns (Figure 3), the most representative being the erosion areas and urban settlements. Erosion dominates Flamengos and Figueira Gorda basins (74.3% and 75.2%, respectively), followed by Poilão (51.5%), Faveta (46.4%), and Saquinho (40.4%). On the contrary, urban settlements were more common in Saquinho (58.2%) and Faveta (44.7%) and lower in Flamengos and Figueira Gorda basins (19.5%). The other classes present insignificant occupations. Even so, Poilão and Faveta basins stand out with higher natural vegetation cover (10.3% and 5.2%, respectively) and agriculture (7.1% and 3.6%, respectively).

3.2. Meteorological Characterization

The difference in the monthly accumulated precipitation between 2016 and the following three years (2017–2019) is evident, with special emphasis on September (241.31 mm) and November (average of the five meteorological stations = 125.21 mm) (Figure 4). In 2016, the total precipitation average was 507.95 mm, much higher than the 30-year average climatic value of 300 mm for the island. However, the situation for the following three years is reversed, with the average annual precipitation less than 300 mm (i.e., 198.88 mm in 2017, 120.44 mm in 2018, and 217.4 mm in 2019). 2018 was particularly dry, especially in the Faveta, Saquinho, and Poilão areas, with total annual precipitation of 68.49 mm, 69.48 mm, and 73.24 mm, respectively. The air temperature presents a similar annual pattern over the four years, with higher temperatures in September and October (28.2 °C and 27.3 °C, respectively).

In the thermal-pluviometric diagram (2016–2020 period), the precipitation greatly exceeds the temperature in September, and only slightly in November, therefore only September and November can be considered wet (Figure 5). Great inter-annual variability was observed, with emphasis on the wet year of 2016, which increased the average precipitation value, especially for September.

3.3. Environmental Parameters: Spatial and Temporal Patterns

3.3.1. Global Trends

The results of the PCA for the first two axes (Figure 6) present eigenvalues of 4.72 and 2.85, respectively, which correspond to an accumulated variance of 44.51%. The first axis explains 27.76% of the total variance and presents a temporal connotation. It opposes the samplings carried out in June and May, mainly at the surface (positive side), to the samplings carried out in October and December, with higher precipitation (PPT). The parameters responsible for this ordination were, for the negative side, HCO₃, TN, NH₄-N, PPT, and Ca; for the positive side, they were CO₃, Na, DO, K, and SO₄. Note that the samples with higher scores on the negative side are from the bottom, which can be explained by the higher values of HCO₃, TN, and NH₄-N, where the effects of precipitation on the input of organic nutrients from the basins are visible. The second axis (16.76% of the total variance) split the samples collected in Saquinho reservoir on the negative side. Moreover, the negative part of the axis contained the Poilão reservoir sampled in October, characterized by higher values of DO, pH, and TP, in opposition to the samples with higher values of Mg, Cl, Si, and Na, mainly from February and December (positive scores on the axis).

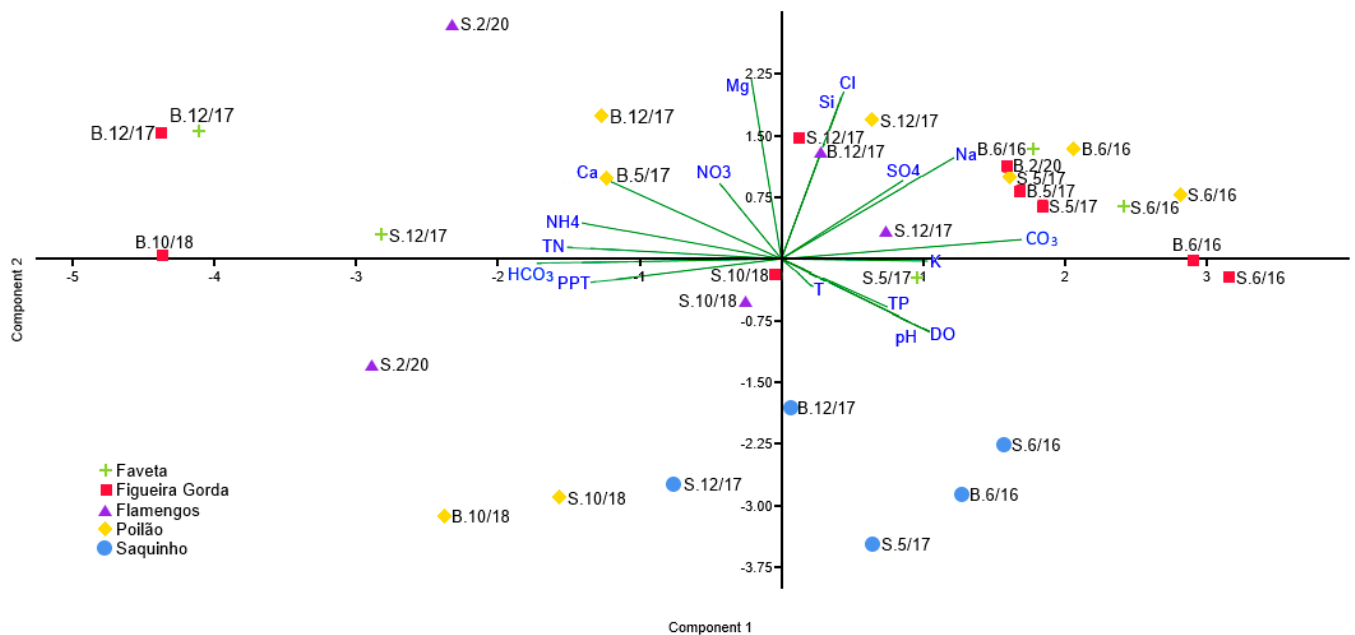


Figure 6. Principal Component Analysis (PCA) biplot for the first two axes, representing the distribution of samples according to environmental gradients. Reservoirs are represented by different shapes and colors, and the codes include S = Surface or B = Bottom samples and the sampling date Month/Year. The codes for the physicochemical parameters are: T—temperature (°C); PPT—monthly accumulated precipitation (mm); TN—total nitrogen; NO₃—nitrates; NH₄—ammonium; TP—total phosphorus; Na—sodium; K—potassium; Ca—calcium; Cl—chlorides; SO₄—sulfates; HCO₃—bicarbonates; CO₃—carbonates; Mg—magnesium; Si—silica; and DO—Dissolved Oxygen.

3.3.2. Spatial Patterns

The results of Kruskal–Wallis tests showed differences among reservoirs only for Ca ($p < 0.05$), Mg ($p < 0.01$), Cl ($p < 0.01$), and SO₄ ($p < 0.01$) (Figure 7). Pairwise Mann–Whitney comparison tests showed that Saquinho presented significantly lower Ca values than Figueira Gorda ($p < 0.05$). For Mg, Saquinho exhibited significantly lower values than all the other reservoirs, (Flamengos ($p < 0.05$), Figueira Gorda ($p < 0.01$), Faveta ($p < 0.05$), and Poilão ($p < 0.01$)). A similar pattern was observed for Cl, with significantly lower values in Saquinho ((Flamengos ($p < 0.05$), Figueira Gorda ($p < 0.01$), and Faveta ($p < 0.01$)), except for Poilão, with no significant differences due to reduced values detected in October 2018. For this same parameter, the Pairwise Mann–Whitney comparison test also revealed significant differences between Figueira Gorda and Faveta reservoirs ($p < 0.01$). Again, for SO₄, Saquinho was significantly different from all the others (Flamengos, $p < 0.05$; Faveta, $p < 0.01$; and Poilão $p < 0.01$), with lower concentrations (exception for Figueira Gorda, with no significant differences due to reduced values detected in October 2018, 0.073 mg SO₄/L, and in December 2020, 14.0 mg SO₄/L). Additionally, for SO₄, Flamengos was significantly different from Faveta ($p < 0.05$) and Poilão ($p < 0.05$), and Figueira Gorda was significantly different from Faveta ($p < 0.05$) and Poilão ($p < 0.05$), both due to comparatively lower values.

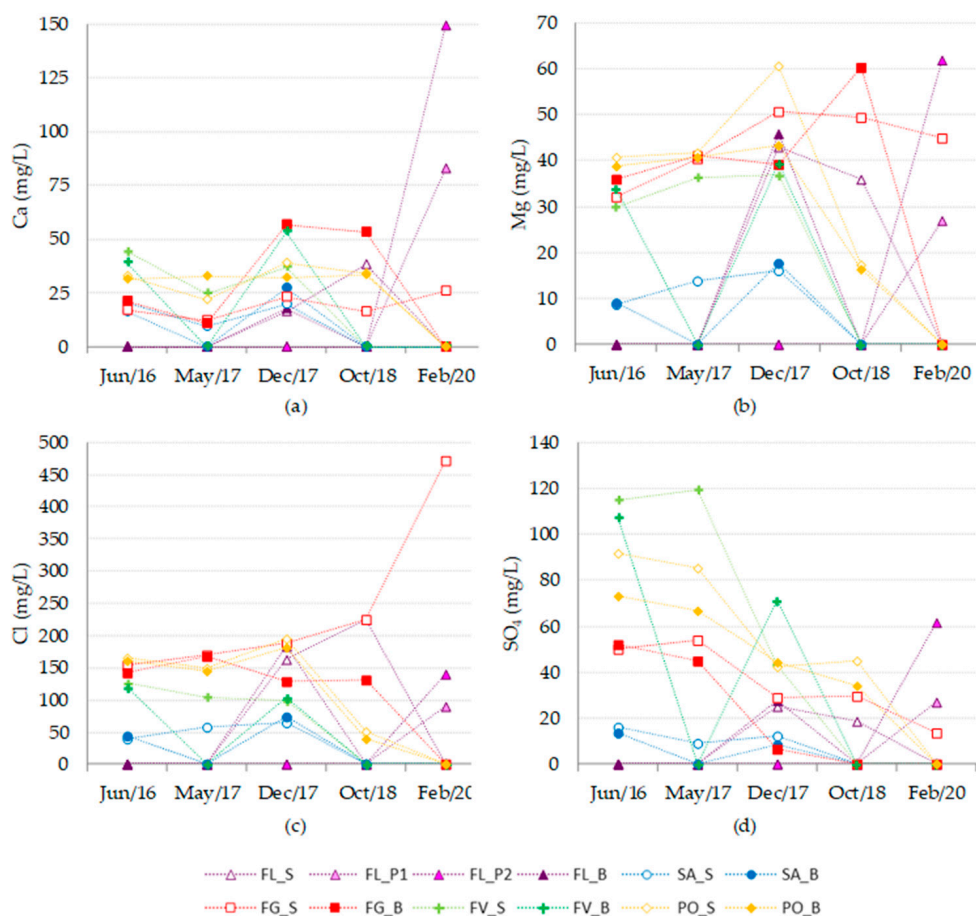


Figure 7. Graphs with the physicochemical descriptors responsible for the significant differentiation among reservoirs (results of Kruskal–Wallis tests): (a) Calcium (Ca, mg/L), (b) magnesium (Mg, mg/L), (c) chlorides (Cl, mg/L), (d) sulfates (SO₄, mg/L). Reservoirs are represented by different shapes and colors, and the codes include FL—Flamengos reservoir, SA—Saquinho reservoir, FG—Figueira Gorda reservoir, FV—Faveta reservoir, PO—Poilão reservoir, S—Surface, B—Bottom, P1—Pool 1, the big pool in Flamengos, P2—Pool 2, the small pool in Flamengos. XX axis show sampling date M/YY.

3.3.3. Temporal Patterns

Figure 8 shows the temporal evolution of the physicochemical parameters that significantly differentiated the five campaigns through the application of Kruskal–Wallis tests (K , $p < 0.001$; HCO_3^- , $p < 0.01$; TN , $p < 0.001$; $\text{NO}_3\text{-N}$, $p < 0.001$; TP , $p < 0.001$; and N:P , $p < 0.05$). For K , June 2016 and May 2017 do not differ from each other, but are significantly higher than December 2017 ($p < 0.05$) and October 2018 ($p < 0.01$). In turn, December 2017 and October 2018 do not differ from each other but are significantly lower than February 2020 ($p < 0.01$ and $p < 0.05$, respectively). For HCO_3^- , June 2016 is significantly lower than December 2017 ($p < 0.05$), October 2018 ($p < 0.01$), and February 2020 ($p < 0.05$). In turn, May 2017 is significantly lower than October 2018 ($p < 0.05$), and December 2017 is significantly lower than October 2018 ($p < 0.05$). In February 2020, there was a larger variability in the magnitude of the data vector (min = 0.0 mg HCO_3^-/L , max = 506.1 mg HCO_3^-/L), and consequently did not differ from any of the other samplings. For $\text{NO}_3\text{-N}$, June 2016 is significantly lower than May 2017 ($p < 0.05$), December 2017 ($p < 0.001$), and October 2018 ($p < 0.001$). Sequentially, May 2017 differs from December 2017 ($p < 0.05$) and October 2018 ($p < 0.01$), and December 2017 is significantly different from October 2018 ($p < 0.01$). Similarly, in February 2020, there is greater variation in the data vector (min = 0.043 $\text{NO}_3\text{-N}$ mg N/L, max = 506.1 $\text{NO}_3\text{-N}$ mg N/L), although not differing from the other sampling campaigns.

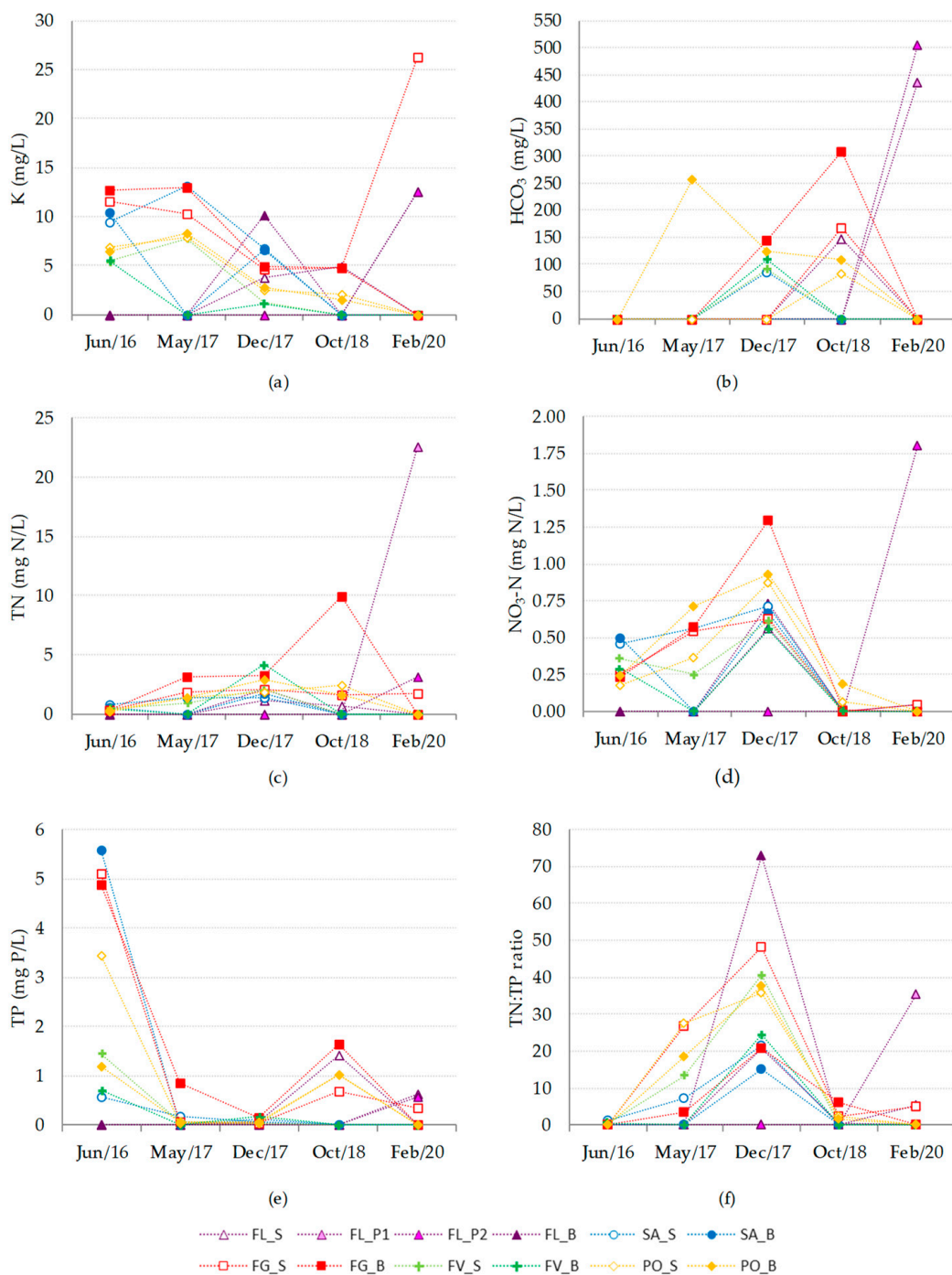


Figure 8. Graphs with the physicochemical descriptors responsible for the significant differentiation among sampling campaigns (results of Kruskal–Wallis tests): (a) K (mg/L), (b) HCO₃⁻ (mg/L), (c) TN (mg N/L), (d) NO₃-N (mg N/L), (e) TP (mg P/L) and (f) TN:TP ratio. XX axis show sampling date M/YY.

For TN, there was a slight increase from June 2016 to December 2017, like that observed for NO₃-N. Only June 2016 is significantly lower than May 2017 ($p < 0.01$), December 2017 ($p < 0.001$), and October 2018 ($p < 0.01$). Contrary to the other parameters, TP showed the greatest magnitude of variation in June 2016. However, the detected concentrations were significantly lower in May 2017 ($p < 0.01$) and December 2017 ($p < 0.001$). In turn, May 2017 is significantly lower than October 2018 ($p < 0.05$), and December 2017 is significantly lower than October 2018 ($p < 0.01$) and February 2020 ($p < 0.01$). Lastly, October 2018 is signifi-

cantly higher than February 2020 ($p < 0.05$). For this parameter, it is important to note that mean values (mean = 1.01 mg P/L and median = 0.45 mg P/L) were very high, well above the maximum recommended value (0.2 mg P/L) by Cape Verdean legislation and above the limit that classifies the systems as eutrophic (0.035 mg P/L). Except for the sampling carried out in December 2017 in the bottom of Flamengos reservoir (0.029 mg P/L), the remaining samples showed concentrations above the eutrophication limit, consequently favorable to primary productivity. The N:P ratio consistently presented very low values for all samples in June 2016 (below 1.4), significantly different from May 2017 ($p < 0.01$), December 2017 ($p < 0.001$), October 2018 ($p < 0.01$), and February 2020 ($p < 0.05$). In May and December 2017, the N:P values were higher and significantly different ($p < 0.05$) from the remaining campaigns. In October 2018, the N:P ratio decreased, being significantly different from June 2016 ($p < 0.01$), May 2017 ($p < 0.05$), and December 2017 ($p < 0.01$). February 2020 presented higher variability among sampled reservoirs, only being significantly different from June 2016.

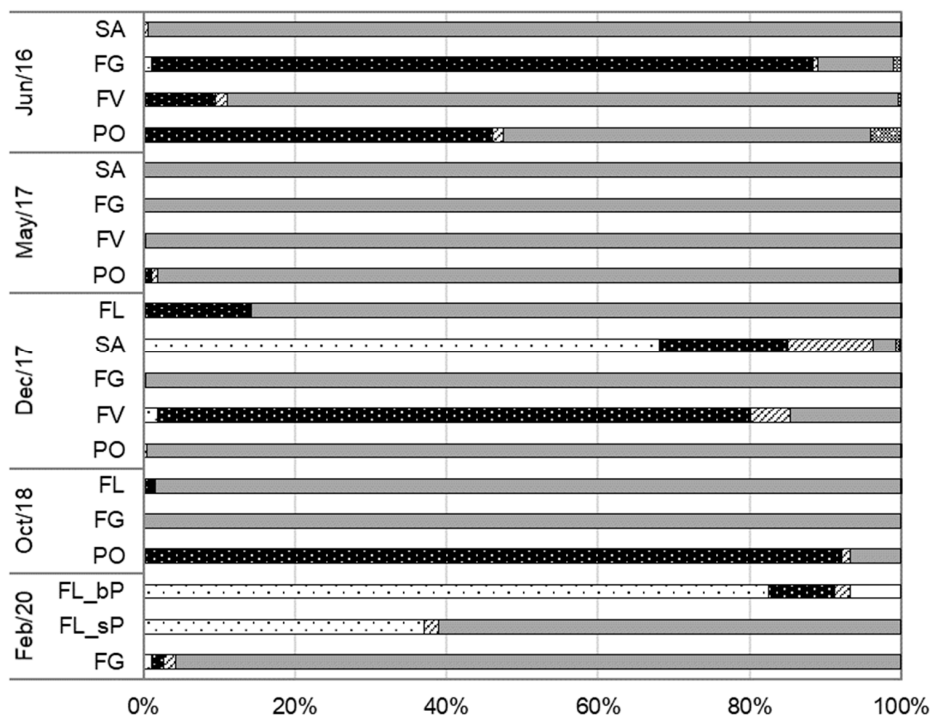
3.4. Phytoplankton

3.4.1. Phytoplankton Assemblages and Diversity

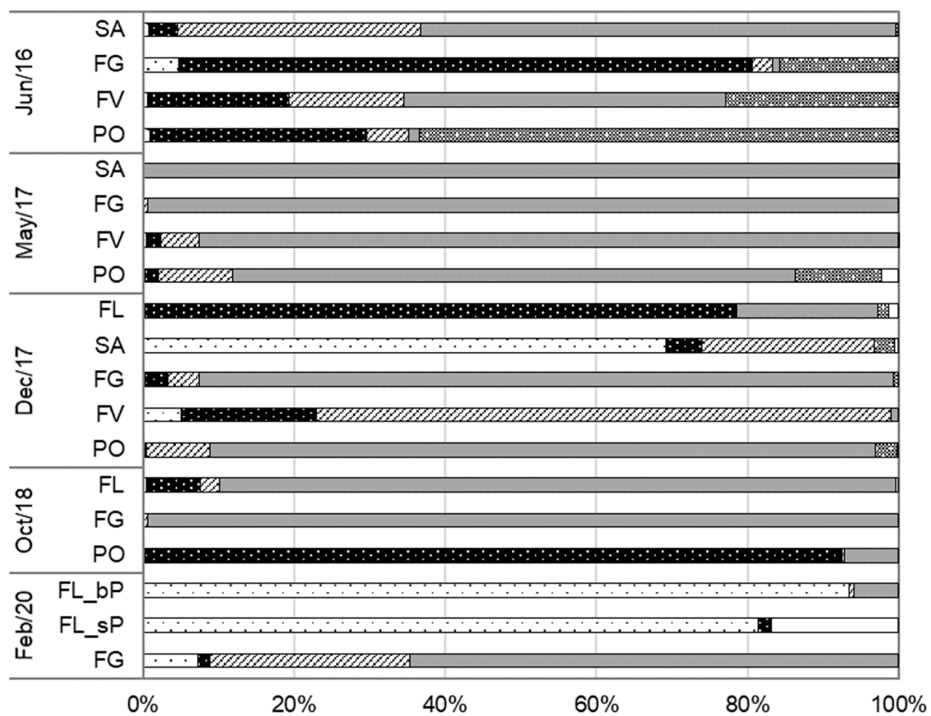
A total of 92 taxa were identified in the dataset (Table S1), from which 46 were present only in one sample and 13 in two samples. These 92 taxa are distributed in 62 genera, from which 17 are Bacillariophyta, 41 are Chlorophyta, 6 are Cryptophyta, 23 are Cyanobacteria, 2 are Dinoflagellata, and 3 are Euglenophyta. Most of the genera comprise only one to three taxa, except for the Chlorophyte genera *Scenedesmus* (seven taxa), *Monoraphidium* (seven taxa), and *Coelastrum* (five taxa), and for the Cryptophyte genus *Cryptomonas* (four taxa). Taxa with the highest relative frequencies were in Chlorophyta, *Tetraedron minimum* (A.Braun) Hansgirg (identified in 73.68% of the samples) and *Scenedesmus communis* E.Hegewald (47.37%); in Cryptophyta, *Cryptomonas erosa* Ehrenberg (63.16%); in Cyanobacteria, *Aphanizomenon* sp. (42.11%) and *Merismopedia tenuissima* Lemmermann (42.11%); and in Dinoflagellata, *Peridinium* sp. (42.11%).

Thirty taxa presented bloom densities (>2000 cells/mL), specifically 2 Bacillariophyta (*Aulacoseira granulata* (Ehrenberg) Simonsen and *Cyclotella* sp.), 9 Chlorophyta (*Coelastrum astroideum* De Notaris, *Crucigenia tetrapedia* (Kirchner) Kuntze, *Kirchneriella* sp., *Monoraphidium contortum* (Thuret) Komárková-Legnerová, *Monoraphidium komarkovae* Nygaard, *Muriellopsis* sp., *Nephrochlamys* sp., *Tetraedron minimum* (A.Braun) Hansgirg, and *Ulothrix* sp.), 4 Cryptophyta (*Cryptomonas curvata* Ehrenberg, *C. erosa* Ehrenberg, *C. ovata* Ehrenberg, and *Komma caudata* (L.Geitler) D.R.A.Hill), and 15 Cyanobacteria (*Anabaena* sp., *Anabaenopsis* sp., *Aphanizomenon aphanizomenoides* (Forti) Hortobágyi & Komárek, *A. manguinii* Bourrelly, *Aphanizomenon* sp., *Coelosphaerium* sp., *Cuspidothrix* sp., *Leptolyngbya* sp., *Merismopedia tenuissima* Lemmermann, *Microcystis* sp., *Oscillatoria limosa* C. Agardh ex Gomont, *Phormidium* sp., *Planktolyngbya limnetica* (Lemmermann) Komárková-Legnerová & Cronberg, *Planktolyngbya* sp., and *Raphidiopsis* sp.).

The relative abundance of phytoplankton group density for all the studied sites showed the dominance of Cyanobacteria in most samples. Exceptions were Figueira Gorda in June 2016, Saquinho and Faveta in December 2017, Poilão in October 2018, and both pools from Flamengos sampled in February 2020 (Figure 9a). With consistent dominance, May 2017 stands out, where Cyanobacteria showed a relative abundance ~100% in all reservoirs, due to blooms of different taxa.



(a)



(b)

Bacillariophyta
 Chlorophyta
 Cryptophyta
 Cyanobacteria
 Dinoflagellata
 Euglenophyta

Figure 9. Relative abundance of phytoplankton groups in density (a) and biovolume (b) for the five reservoirs along the studied period (June 2016–February 2020). FL—Flamengos reservoir; FL_bP—big pool in Flamengos reservoir; FL_sP—small pool in Flamengos reservoir; SA—Saquinho reservoir; FG—Figueira Gorda reservoir; FV—Faveta reservoir; PO—Poilão reservoir.

Thus, in Faveta, the dominance is due to two taxa, *Aphanizomenon aphanizomenoides* (100,923 cells/mL) and *Planktolyngbya* sp. (295,560 cells/mL). In Figueira Gorda, it is also due to two taxa, *Aphanizomenon manguinii* (939,863 cells/mL) and *Microcystis* sp. (413,511 cells/mL). In Poilão, it is due to a bloom of *Aphanizomenon* sp. (62,937 cells/mL). In Saquinho, it is due to three taxa, *Anabaenopsis* sp. (160,021 cell/mL), *Microcystis* sp. (5,183,352 cells/mL), and *Phormidium* sp. (28,700 cells/mL). Although less frequently, the dominance of other taxonomic groups was observed, namely Chlorophyta in Figueira Gorda in May 2016, in Faveta in December 2017, and Poilão in October 2018, with blooms of *Tetraedron minimum* (16,627 cells/mL), *Muriellopsis* sp. (27,282 cells/mL), and *Coelastrum astroideum* (20,818 cells/mL). Regarding Bacillariophyta, although present in low numbers in most samples, they were dominant in Saquinho in December 2017 through two taxa, *Aulacoseira granulata* (8726 cells/mL) and *Cyclotella* sp. (17,497 cells/mL). The Cryptophyta, Dinoflagellata, and Euglenophyta were present in low abundances, contributing only slightly to the overall productivity of the studied systems.

Cryptophyta and Dinoflagellates gain relevance when relative biovolume is considered (Figure 9b). Cryptophyta stands out in Saquinho in June 2016 (32.2%) and December 2017 (22.2%), and in Faveta in December 2017 (76.1%); and Dinoflagellates in June 2016 in Figueira Gorda (15.7%), Faveta (22.8%), and especially in Poilão (63.5%). For Chlorophytes, the situation also changes, especially in Flamengos in December 2017 (78.5%). The Bacillariophyta also assume higher relative biovolume, with special emphasis on the pools in Flamengos, February 2020 (pool 1, 81.4%; pool 2, 93.5%). Euglenophytes, although never dominant in the phytoplankton community, gain relevance, especially in pool 1 (“big pool”) in Flamengos in February 2020 (16.8%).

The nMDS analysis (Figure 10) presented a stress level of 0.18, below the limit of 0.2 for a potentially useful 2D representation. This 2D ordination revealed that phytoplankton samples are not grouped by reservoirs (Figure 10a), a result also confirmed by ANOSIM with no significant differences detected (Global $R = 0.074$) (Table S2). Contrariwise, samples are grouped by months (Figure 10b). This result was further confirmed by ANOSIM ($R = 0.556$, $p < 0.001$) (Table S2), revealing significant differences despite the low average similarity within months (between 8.57% and 0.26%), indicating that the detected difference among months is not very robust. Moreover, no significant differences were identified between June 2016/May 2017, and December 2017/June 2016.

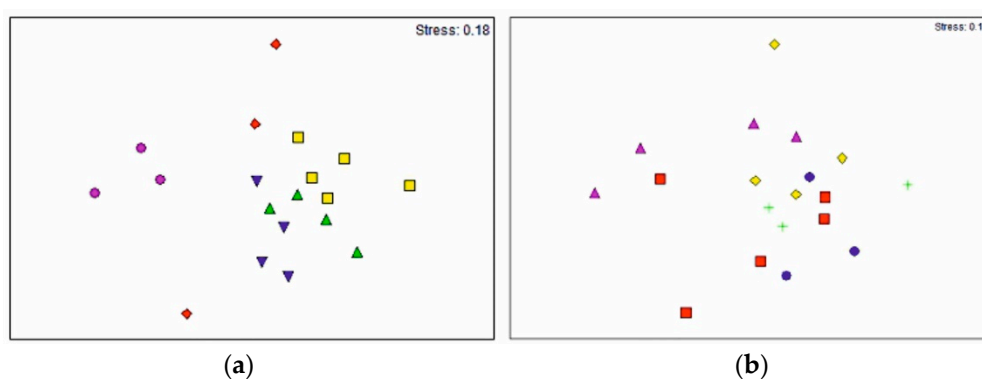


Figure 10. 2D non-metric multidimensional scaling ordination plot of samples based on phytoplankton assemblages, with identification of reservoirs (a) and sampling months (b). (a) ▲ Flamengos reservoir; + Faveta reservoir; ■ Figueira Gorda reservoir; ● Saquinho reservoir; ◆ Poilão reservoir. (b) ▲ June; ▼ May; ■ December; ● February; ◆ October.

The SIMPER analysis for the sampling months revealed that *Tetraedron minimum* (Chlorophyte) and *Raphidiopsis* sp. (Cyanobacterium) were indicators for June 2016, despite the low average similarity value (Table S3). *Tetraedron minimum*, which contributed 88.65% to the similarity of the group, was present in the Faveta, Figueira Gorda, and Poilão reservoirs. *Raphidiopsis* sp. (3.4% contribution to similarity) was only present in the

Figueira Gorda and Poilão reservoirs. The Cyanobacteria *Aphanizomenon aphanizomenoides*, *Planktolyngbya* sp., and *Microcystis* sp. were indicators for May 2017, with very high abundances. The first two taxa were present in Faveta and Poilão reservoirs with concentrations of high and moderate risk levels (see 3.4.2 Risk Levels of Toxic Cyanobacteria Occurrence). *Microcystis* sp. was present in Figueira Gorda and Saquinho reservoirs, also with very high levels (i.e., high risk to human health, >100,000 cells/mL). May 2017 is separated from the other months only by Cyanobacteria taxa. *Planktolyngbya limnetica*, which contributed 72.2% to the similarity average of December 2017, was present in Faveta, Figueira Gorda, Saquinho, and Flamengos. The second indicator taxon for this sampling month was *Cryptomonas erosa* (13.81%), a Cryptophyte present in all the reservoirs. *Aphanizomenon* sp. was also an indicator in December 2017, despite its low contribution to the similarity of the group (7.1%). For October 2018, similarity is attributed to *Scenedesmus communis* E.Hegewald, *Coelastrum astroideum*, and *Scenedesmus acutus* Meyen (Chlorophyta). February 2020 is characterized by a greater number of indicator taxa, namely, one Cyanobacterium (*Planktolyngbya* sp.) and five Bacillariophyta (i.e., *Navicula veneta* Kützing, *Caloneis bacillum* (Grunow) Cleve, *Nitzschia palea* (Kützing) W.Smith, *Eolimna subminuscula* (Manguin) Gerd Moser, Lange-Bertalot & Metzeltin, and *Tryblionella apiculata* W.Gregory). In fact, February 2020 corresponds to a period of extreme drought; Faveta, Poilão, and Saquinho reservoirs were dry, Figueira Gorda had very little water (less than 4 m depth), and the Flamengos reservoir was also dry, with the exception of the two pools fed by groundwater. In these systems, the total density was much lower than that detected in previous months (3079 cells/mL in Figueira Gorda, 3067 cells/mL in pool 1 “big pool” and 1614 cells/mL in pool 2 “small pool”), and the community had fewer Cyanobacteria and a great diversity of Bacillariophyta, with special emphasis on *Navicula veneta*, *Caloneis bacillum*, and *Eolimna subminuscula*, present in the three sampling sites (Table S3). It should also be noted that the average similarity of the indicator taxa was very low, which shows little robustness in the individualization of months.

Descriptive statistics of different phytoplankton diversity metrics and indexes calculated for the studied reservoirs are presented in Table 4.

Table 4. Phytoplankton diversity metrics of the studied reservoirs; median (interquartile range) values are presented.

Metrics	Faveta	Figueira Gorda	Poilão	Saquinho	Flamengos
N° of Taxa (S)	10.0 (9.5–13.0)	9.0 (8.0–11.0)	15.0 (13.3–16.0)	15.0 (12.0–19.5)	11.5 (10.5–14.0)
Density (N)	4.0×10^5 (2.2×10^5 – 4.0×10^5)	1.2×10^5 (2.0×10^4 – 1.4×10^6)	2.9×10^5 (11×10^5 – 7.5×10^5)	5.4×10^6 (2.7×10^6 – 5.9×10^6)	3.2×10^5 (2.5×10^3 – 7.9×10^5)
Biovolume (Bv)	10.68 (7.25–25.0)	7.58 (6.02–40.60)	3730.00 (19.91–58.92)	111.99 (71.02–158.70)	6.47 (1.22–18.42)
Shannon Index (H')	0.93 (0.76–1.07)	0.60 (0.60–0.62)	0.94 (0.66–0.130)	0.17 (0.11–0.96)	1.19 (0.57–1.84)
Margalef (M)	0.76 (0.73–0.96)	0.75 (0.57–0.87)	1.03 (0.89–1.23)	0.89 (0.70–1.53)	1.31 (1.11–138))
Evenness (J)	0.42 (0.43–0.26)	0.28 (0.26–0.32)	0.35 (0.25–0.49)	0.08 (0.05–0.31)	0.53 (0.23–0.81)
Dominance (D)	0.59 (0.51–0.60)	0.64 (0.59–0.70)	0.57 (0.45–0.64)	0.93 (0.60–0.96)	0.47 (0.22–0.74)

Overall, no significant differences were obtained among reservoirs and sampling months for phytoplankton diversity metrics/indexes. In fact, the median for α diversity is similar among reservoirs (Table 4). In Figure 11, Figueira Gorda sampled in October 2018 stands out with the lowest α diversity, as does Saquinho in December 2017 with the highest value. This was also the reservoir that showed the highest average density (median = 5,372,280 cells/mL) (Table 4). H' showed very low values for all reservoirs (Table 4), and the highest value was observed in February 2020 in an extreme drought situation. The same pattern was observed for M, with the highest value recorded in Saquinho in December 2017. Noteworthy are the extremely high D and low J values observed in the

Saquinho in May 2017, in a situation with a relative abundance of Cyanobacteria close to 100%. No strong correlations were found between different diversity metrics/indexes and environmental variables. However, M showed a positive correlation with Ca ($r = 0.599$, $p < 0.01$). D presented negative correlations with Ca ($r = -0.47$, $p < 0.05$), SO_4 ($r = -0.470$, $p < 0.05$), and HCO_3^- ($r = -0.476$, $p < 0.05$). Complementarily, J revealed a positive correlation with HCO_3^- ($r = 0.526$, $p < 0.05$) and a negative correlation with CO_3 ($r = -0.483$, $p < 0.05$). Evenness J also showed a positive correlation with Total P ($r = 0.475$, $p < 0.05$). In turn, N presented a negative correlation with Total P ($r = -0.49$, $p < 0.05$) and HCO_3^- ($r = -0.582$, $p < 0.01$).

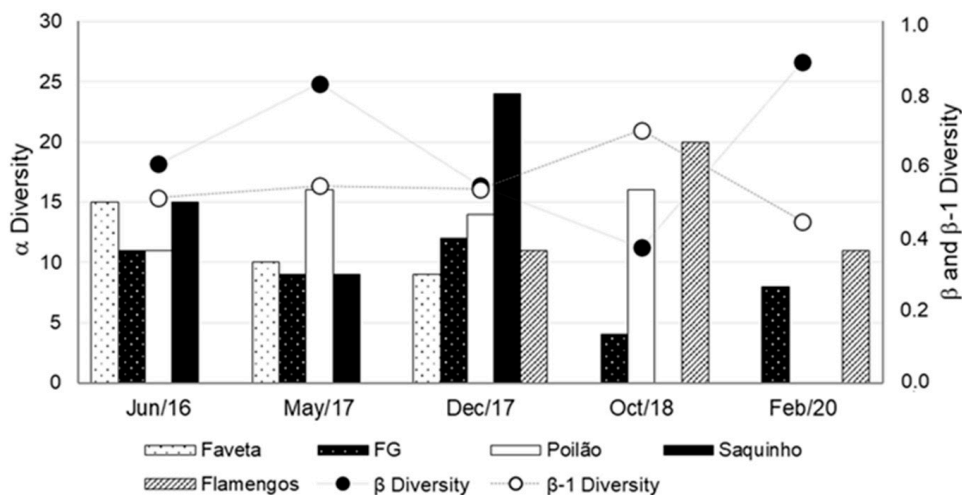


Figure 11. α diversity per reservoir over the study period. Evolution of β diversity based on the similarity index (Sorensen index) and on the dissimilarity index.

The α diversity and β diversity throughout the study period are presented in Figure 11. The Sorensen β diversity and $\beta-1$ diversity show an inverse evolution pattern, related to their characteristics (β diversity is a similarity index [77] while $\beta - 1$ diversity is a dissimilarity index). May 2017 and October 2018 are the months with the most distinct communities, evident in the similarity index values for both months and the dissimilarity index value for October 2018. It should be noted that October corresponds to the wet period, where the effect of precipitation (albeit reduced), together with the high temperatures recorded (27.3 °C average value), may have contributed to the differentiation of communities among reservoirs. In fact, the phytoplankton communities of Figueira Gorda and Flamengos were dominated by Cyanobacteria (99.90% and 98.52%, respectively), while in Poilão, the phytoplankton was dominated by chlorophytes (92.0%). December 2017 also presented lower similarity (measured by the Sorensen index), given the higher value of α diversity recorded in the Saquinho reservoir (24 taxa).

The γ diversity, presented in Figure 12, reveals that Bacillariophyta, Chlorophyta, Cryptophyta, Cyanobacteria, and Euglenophyta were present in all samples (although with different diversities), which was not observed for Dinoflagellata (absent in the samples of October 2017 and February 2020). Chlorophyta is the most represented group, followed by Cyanobacteria with the exception of February 2020, with greater representation of Bacillariophyta. The highest γ diversity was detected in December 2017, related to the highest representativeness of Chlorophyta, whilst the lowest values were detected in February 2020.

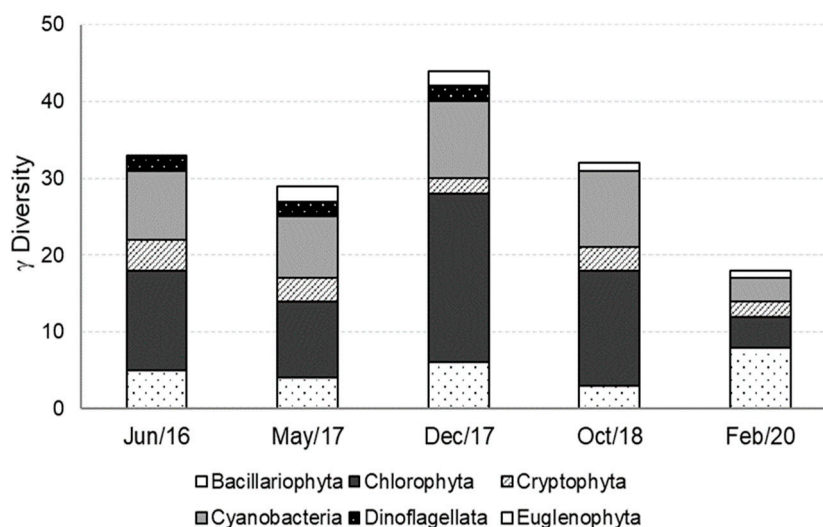


Figure 12. Regional γ diversity of the five reservoirs per sampling month, distributed by taxonomic classes.

3.4.2. Risk Levels of Toxic Cyanobacteria Occurrence

The Cyanobacteria taxa present in each reservoir, as well as their cell density and the relative abundance for the month of occurrence, are presented on Table S4.

In all reservoirs, bloom densities (above 2000 cells/mL) were detected. *Aphanizomenon* sp. appeared in a bloom situation in 26.3% of the total samples; *Microcystis* sp. and *Planktolyngbya limnetica* shaped blooms in 21% of samplings. With a relative frequency of 15.7%, *Aphanizomenon aphanizomenoides*, *A. manguinii*, and *Planktolyngbya* sp stand out; *Raphidiopsis* sp. was present twice in a bloom situation; and those with a bloom in a single sample are *Anabaena* sp., *Anabaenopsis* sp., *Coelosphaerium* sp., *Cuspidothrix* sp., *Leptolyngbya* sp., *Merismopedia tenuissima*, *Oscillatoria limosa*, *Phormidium* sp., and *Planktothrix agardhii* (Gomont) Anagnostidis & Komárek.

Additionally noteworthy are certain taxa that were present with a relative abundance greater than 50% and extremely high densities (above or close to 100,000 cells/mL): *Aphanizomenon aphanizomenoides* (Faveta in June 2016, Poilão in May 2017), *A. manguinii* (Figueira Gorda October 2018), *Coelosphaerium* sp. (Flamengos in October 2018), *Cuspidothrix* sp. (Poilão in December 2017), *Planktolyngbya limnetica* (Saquinho in December 2017), *Planktolyngbya* sp. (Faveta in May 2017, Figueira Gorda in December 2020), and *Microcystis* sp. (Figueira Gorda in December 2018, Saquinho in June 2016 and May 2017).

Additionally, the significant correlations obtained between Cyanobacteria (both in terms of cells density and biovolume) and diversity metrics/indexes are indicators of the global dominance of these organisms (Table 5). Except for α diversity (S), all the other metrics and indexes showed significant correlations, positive with D (both for Cyanobacteria N and Bv) and obviously negative with H' M (this one only Cyanobacteria N), and J .

Table 5. Spearman correlation between Cyanobacteria density (N). Cyanobacteria biovolume (BV) and diversity metrics. Significant p values (* $p < 0.05$. ** $p < 0.01$. *** $p < 0.001$) are presented.

Metric	Cyanobacteria Density (N)	Cyanobacteria Biovolume (BV)
N° of Taxa (S)	0.032	0.131
Density (N)	0.970 ***	0.936 ***
Biovolume (Bv)	0.950 ***	0.810 ***
Dominance (D)	0.688 **	0.591 **
Shannon Index (H')	−0.753 ***	−0.683 ***
Margalef (M)	−0.542 *	−0.429
Evenness (J)	−0.813 ***	−0.748 ***

According to the cyanobacteria cell-based criterion [78], all reservoirs presented a risk level, with more than 50% of samples carried out in a high-risk situation (Figure 13a). Moderate risk was only detected in Figueira Gorda and Poilão, with all reservoirs showing at least one sampling carried out in a low-risk situation. Flamengos was the only reservoir that presented a single no-risk situation.

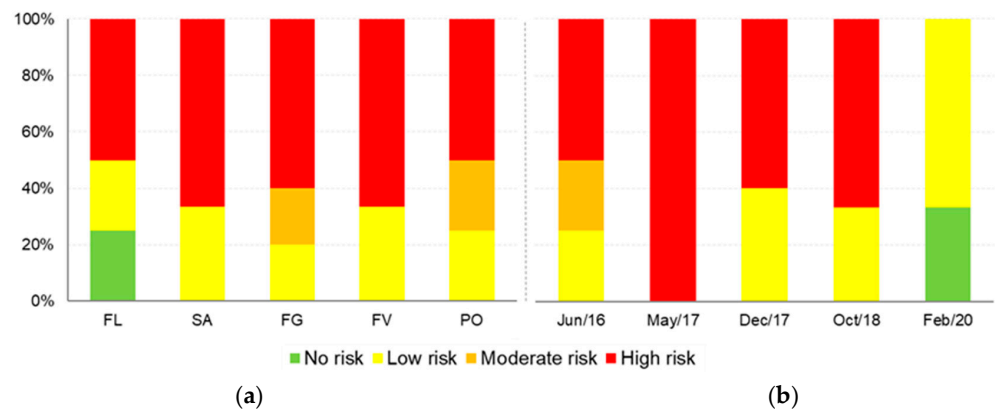


Figure 13. Risk levels of the five studied reservoirs (a) and sampling months (b) for cyanobacteria cell density. FL—Flamengos reservoir; SA—Saquinho reservoir; FG—Figueira Gorda reservoir; FV—Faveta reservoir; PO—Poilão reservoir.

Regarding the sampling periods (Figure 13b), May 2017 and February 2020 stand out from the rest. In May 2017, all the samplings were realized in a high-risk situation (above 100,000 cells/mL). February corresponds to the period with lower risk conditions, integrating the sampling carried out in pool 2 “small pool”, with no cyanobacteria.

Melting curve analyses for each reservoir and different target genes (see Table 3) are presented in Figure 14. For Flamengos (a), both in October 2018 and in small pool 2 in February 2020, the melting curves surpass the baseline, indicating that the presence of Cyanobacteria was detected (a1). Nevertheless, none of the other toxin-producing genes were detected in either October 2018 or February 2020. For Figueira Gorda, the presence of Cyanobacteria was detected in October 2018 and February 2020 (b1). On the contrary, in Poilão, none of the target genes were detected (c1–c5). In Figueira Gorda, sampled in October 2018, all the target genes responsible for the presence of Cyanobacteria and toxin-producing genes such as Microcystins, Nodularins, and Cylindrospermopin (b1–b5) were present. In the same reservoir, in February 2020, the presence of Cyanobacteria was detected, as well as the presence of toxin-producing genes of Microcystins, Nodularins, and one gene responsible for cylindrospermopsin production (Polyketide synthetase).

3.4.3. Relationship between Environmental Variables and Phytoplankton Descriptors

Of all the phytoplankton metrics, multiple regression models with environmental descriptors were only found for the total biovolume, Bacillariophyta, Chlorophyta, and Cyanobacteria densities (Table 6). The total biovolume was related to geological influence variables (Na, Mg, and HCO_3), T, and $\text{NO}_3\text{-N}$. The density of Bacillariophyta was negatively related to CO_3 and PPT. The density of Chlorophyta seems to also be dependent on geological influence variables (K and HCO_3) as well as on nitrogen (TN and $\text{NH}_4\text{-N}$), showing a negative relationship, probably due to their assimilation and transfer to the algal biomass. The density of Cyanobacteria was related to Na (geological influence) and TP (although negatively due to its assimilation), with a high coefficient of determination ($R^2 = 0.71$). It should be noted that the coefficients of determination were relatively high (greater than 0.50), especially for the total biovolume and density of Cyanobacteria. The lower coefficients of determination observed in the models for Bacillariophyta and Chlorophyta, and the non-existence of significant models for the other phytoplankton metrics,

can be related to the fact that the analyzed environmental parameters do not constitute the only determinant or explanatory descriptors of the phytoplankton.

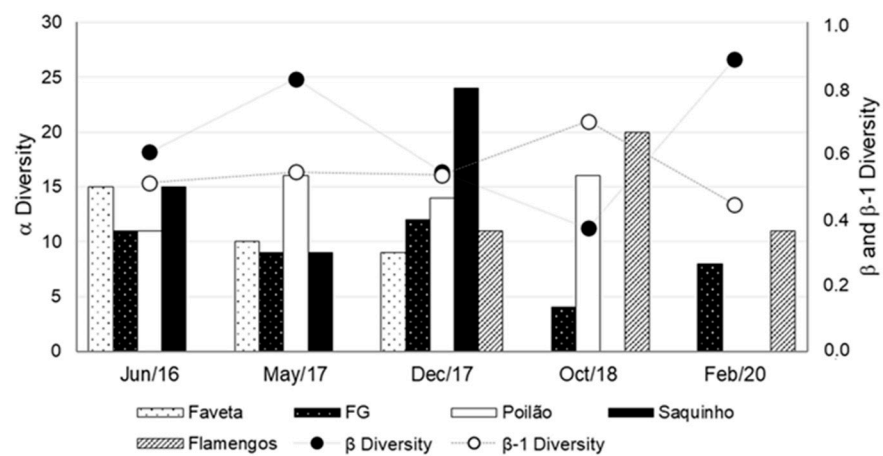


Figure 14. Melting curves for the different reservoirs. Flamengos (a), Figueira Gorda (b), Poilão (c) (each curve represents a sampling date) and different target genes. (1) shows the gene that identifies the presence or absence of Cyanobacteria (16 rRNA gene), (2) presence or absence of Microcystin-producing gene (mcyB), (3) presence or absence of nodularin-producing gene (mcyE/nda), (4,5) presence and absence of cylindrospermopsin-producing genes (Peptide synthetase) and polyketide synthetase, respectively.

Table 6. Summary results of multiple regression analysis applied to phytoplankton determinant descriptors. Significant p values (* $p < 0.05$ ** $p < 0.01$ *** $p < 0.001$) are presented. D.F.—Degrees of Freedom.

Dependent Variable	Independent Variables	Regression Coefficient	F Value	R ²	D.F.
Total biovolume	Na	1.77 *	19.34	0.84	18
	Mg	−1.71 **			
	NO ₃ -N	4.56 ***			
	HCO ₃	−0.21 *			
	T	8.58 ***			
Density of Bacillariophyta	CO ₃	−0.61 **	12.11	0.55	18
	PPT	−2.66 ***			
Density of Chlorophyta	K	−3.49 ***	10.20	0.67	18
	NH ₄ -N	−13.17 *			
	HCO ₃	−0.43 *			
	TN	−4.13 *			
Density of Cyanobacteria	Na	5.79 **	23.42	0.71	18
	TP	−3.77 ***			

4. Discussion

4.1. Environmental Parameters: Spatial and Temporal Patterns

The physicochemical results revealed that the reservoirs differed significantly only for the predominantly geological influencing variables (Ca, Mg, Cl, SO₄), and that the Saquinho reservoir tended to have lower concentrations of Ca, Mg, Cl, and SO₄. This reservoir is in the middle zone of the Charco stream, under the geological influence of the Assomada Formation, made up of mantles, drainages, and basaltic pyroclasts, comparatively poorer in mineral elements than the other geological units where the other reservoirs are located [90]. Some authors refer to the relevance of natural geological and biological processes as sources of nutrients to aquatic ecosystems [91–94], adding that catchment water quality varies spatially with geology and soils [95].

The reservoirs were not different according to organic variables, which can be explained by the high concentrations of P and N recorded in the five reservoirs above the Cape Verdean legislation and the limit that classifies the systems as eutrophic. The high levels of P and N in the water seem to be mainly due to the LULC, understood to be responsible for water quality degradation by several authors [96–100]. In the study basins, the high levels of P and N may be mainly attributed to the large occupation of erosion areas (to which semi-arid lands are highly susceptible) and urban settlements [101–103].

The torrential precipitation regime can transport large quantities of sediment, especially when the cover needed to protect the soil from wind and water erosion is not complete, characterizing source-limited denudation, with more material transported than detached in an erosion scenario [104]. This erosion hazard during drought events can increase with prolonged grazing pressure, reducing the plant cover [102,105–107]. Noteworthy are the Flamengos and Figueira Gorda reservoirs with more than 70% erosion areas, and Saquinho, Faveta, and Poilão, with urban settlements representing more than 30%. On the other hand, in the municipalities where the reservoirs are located, most of the population is not connected to the public sewer network nor to the evacuation system of solid wastes. Consequently, the water in the reservoirs reflects this situation, which is aggravated in wet periods due to the torrential regime of precipitation. This observation is evident for TP, which tended to have higher concentrations in June 2016 and October 2018, with a consequent decrease in the N:P ratio. Although June corresponds to the dry period, 2016 was classified as a wet year, which may be related to the higher concentration of TP in the water and also to the greater variation in the data vector, since precipitation varies regionally. Consequently, the respective erosion and nutrient input, resulting from the torrential precipitation regime in a source-limited denudation situation characteristic of semi-arid regions [103–108], is also variable. October 2018, in turn corresponding to the wet period and the highest TP concentration detected (also coinciding with consistently lower N:P values), may also be related to the external input resulting from soil erosion and the carryover from waste solids and effluents produced in the basin.

A similar pattern is not, however, detected for TN and $\text{NO}_3\text{-N}$, with an increasing trend from June 2016 to December 2017 and a decrease in October 2018. In October 2018, coinciding with lower $\text{NO}_3\text{-N}$ concentrations, a bloom of *Aphanizomenon manguinii* (N_2 -fixing taxa) was recorded in Figueira Gorda. On the contrary, in Flamengos, a bloom of *Coelosphaerium* sp. (non- N_2 -fixing Cyanobacteria) was identified, and Chlorophyte blooms were registered in Poilão (*Coelastrum astroideum*), which globally, may have contributed to a decrease in $\text{NO}_3\text{-N}$ and TN available in the water in these two reservoirs.

The temporal dynamics were mainly dictated by precipitation, which showed a large variation over the studied period, being inversely related to the temperature, which evidenced a similar annual pattern (Figure 4). 2016 corresponded to a wet year followed by three extremely dry years (2017, 2018, and 2019). It should be noted that in 2018, the Saquinho, Faveta, and Poilão reservoirs were completely dry, and in February 2020, the Flamengos reservoir only presented water in two remaining pools, dug by the local population to extract water from underground sources. In this transported-limited situation, with more material detached than carried away (sensus Ahnert, 1998), the available P released from sediments could be quickly absorbed by the phytoplankton, which can be inferred from the low N:P ratio values detected in the Figueira Gorda reservoir and in the small pool of the Flamengos reservoir.

Overall, the physicochemical variables that significantly differentiated the sampling campaigns, with higher values in February 2020 (peak of drought) in Flamengos (big pool), were HCO_3 , due to the influence of groundwater, and TN and $\text{NO}_3\text{-N}$, due to the organic contamination of waste, resulting from its use by the population. In the dry period, it is common practice in Cape Verde for the local population to invade dry areas within the reservoirs and practice subsistence agriculture. This fact was verified in Poilão, Faveta, Figueira Gorda, and Flamengos reservoirs.

The PCA analysis did not differentiate the reservoirs for the overall environmental variables, which is in agreement with the results of the Kruskal–Wallis tests (i.e., reservoirs only differed due to their geological characteristics), revealing no significant differences for organic pressure indicator variables. Both axes presented temporal significance. The first axis differentiated the samplings according to rainfall and the parameters that may have entered the systems from the drainage basins (TN and NH₄-N). The second axis separated Saquinho from the other reservoirs, due to the different geological characteristics of the basin. It should be noted that over the study period, the water depth and the availability of water in the reservoirs were decreasing, which is why no separation was detected between surface and bottom samplings.

4.2. Phytoplankton

4.2.1. Phytoplankton Assemblages and Diversity

Considering the level of eutrophication registered, the preponderance of Cyanobacteria in all reservoirs is not surprising, since one of the most visible and the well-known changes associated with eutrophication is the mass development of these organisms [109–114]. Cyanobacteria emerged with very high densities, dominating the phytoplankton community globally for the five reservoirs in May 2017. However, the taxa responsible for this dominance were not the same in all reservoirs, particularly for May 2017 but also for the other sampling periods. An observation that can be explained in light of the metacommunity ecology, which addresses local communities as sets of habitat patches interconnected by dispersal processes [115,116], is focused on how and to what extent organisms drive the structure of these metacommunities, emphasizing the dominant role of local habitat factors on community composition and biodiversity [110,117,118].

Less frequently, taxa belonging to other algal groups were also dominant, particularly Chlorophyta and Bacillariophyta. In terms of biovolumes, other groups gained relevance, particularly the Cryptophyta, specifically in Faveta in December 2017 where they were dominant.

nMDS and ANOSIM analyses showed that phytoplankton is not grouped by reservoirs, with a more consistent grouping for the sampling periods. However, the average of similarity within months was low, which indicates slight internal cohesion, explained by the variability of the dominant taxa within reservoirs. Similarly, the SIMPER analysis, used to identify characteristic taxa of the groups validated by ANOSIM (i.e., sampling months), showed low average similarity values, which reveals little robustness of these taxa indications. In other words, although there are differences among sampling months, the resulting temporal succession is not very strong, which is probably due to the drought in 2017, 2018, and 2019 that tended to homogenize communities [119,120]. In June 2016, with greater water availability, the indicator taxon was Chlorophyta (*Tetraedron minimum*), which bloomed in the Faveta, Figueira Gorda, and Poilão reservoirs; in May 2017, the indicator taxa were only Cyanobacteria, given the dominance of this group in all reservoirs. Again, in the wet period (October 2018), the indicator taxa were all Chlorophytes, which in some reservoirs were also blooming. The rainfall seems to have contributed to the community structure change in some reservoirs, breaking the dominance of Cyanobacteria. On the contrary, during the peak of the drought (February 2020), Bacillariophyta in the two pools fed by groundwater (located inside Flamengos reservoir) stood out as dominant. In this context, [110] found that the influence of eutrophication on phytoplankton is dependent on system size and that differences in the dynamics of key species and community composition are to be expected.

Strong correlations between the different diversity metrics/indexes and environmental variables were not detected. However, some correlations with geological influence variables stood out (Ca, SO₄, HCO₃, and CO₃), which basically differentiate Saquinho, located on a distinct geological unit (Assomada Formation, AF), from the other reservoirs. The positive correlation between *J* and the phytoplankton density and the negative correlation between the phytoplankton density and TP were also highlighted. The influence

of TP in the distribution of species can be explained by its rapid assimilation in bloom situations, consequently presenting a negative correlation with phytoplankton density, despite the high levels of TP concentrations above 0.035 mg/L (the limit of eutrophication). This means that even in situations with high N:P ratios, TP does not limit the phytoplankton development (only in December 2017 in the bottom of Flamengos reservoir, the TP concentration was lower than 0.035 mg/L).

The two β -diversity indexes emphasize complementary aspects in the succession of taxa over time and are important for understanding the temporal dynamics in a universe that progressively lost representation due to extreme drought. Both indices highlight October as the period that showed more distinct communities, probably related to the higher TP concentration from the basin, owing to the influence of precipitation. In fact, the phytoplankton assemblages of Figueira Gorda and Flamengos were dominated by Cyanobacteria, while in Poilão, phytoplankton was dominated by chlorophytes. The Sorensen index also shows greater similarity in May 2017, which is mainly due to the dominance of Cyanobacteria in all reservoirs with a high percentage of common taxa among reservoirs. In accordance with a β -diversity concept [121], species turnover implies the replacement of species as a consequence of environmental changing, and systems with high β diversities usually have a higher conservation value [122]. The wet period causes a change in the community, which is reflected differently in each reservoir (great dissimilarity), being fundamental for a renewal of the community structure. The γ diversity was utilized to measure reservoir phytoplankton richness at the Santiago Island macro-scale [123]. Our findings point to Chlorophytes having the greatest taxonomic richness in all periods, apart from February 2020, when Bacillariophyta was dominant in the community. The preponderance of Chlorophytes richness is common in lentic environments, regardless of their trophic level and nutrient concentration, as this class is characterized by high morphometric and physiological variability, allowing adaptability to a wide variety of conditions [124,125]. Cyanobacteria is the group with the second greatest taxonomic richness, in a proportion equivalent to approximately half of that recorded for Chlorophytes. N:P < 22 was adopted by [126] to describe Cyanobacteria dominance, since these organisms can compete for nitrogen better than other phytoplankton groups. Thus, in situations with excessive P loading, nitrogen becomes scarce, and cyanobacteria are predicted to be dominant. In fact, 72% of the total analyzed samples presented N:P ratios < 22, which demonstrates conditions for Cyanobacteria dominance. Nevertheless, the taxa variation/replacement in Santiago reservoirs seems to be the predominant mechanism in shaping phytoplankton γ diversity. In this sense, these organisms do not experience dispersal limitation [127] and their biogeographic patterns reflect current environmental conditions, regardless of the geographic distance among systems [128], in accordance with the statement that the biogeographic distribution of microorganisms is under the view of '*Everything is everywhere, but the environment selects*' [129,130].

4.2.2. Risk Levels of Toxic Cyanobacteria Occurrence

The results showed that all reservoirs presented Cyanobacteria with high densities and relative abundance greater than 50%. However, only Figueira Gorda bloomed in all sampling periods, although with different risk levels. The taxa responsible for blooms and risk levels were also different among reservoirs and sampling months, making it difficult to establish a scenario for the occurrence of a certain taxon. However, in global terms, of the 23 identified Cyanobacteria, 74% showed at least one bloom episode.

Regarding TP concentration, all reservoirs are eutrophic, which explains the high density of Cyanobacteria, with the dominance of potentially toxin-producing genera (e.g., *Anabaenopsis*, *Aphanizomenon*, *Coelosphaerium*, *Dolichospermum*, *Microcystis*, *Oscillatoria*, *Phormidium*, *Planktothrix*, and *Raphidiopsis*), already reported in several areas around the world [12,13,131–137]. Therefore, in all reservoirs, high-risk situations were identified, especially considering the identified taxa are potential producers of different toxins, namely microcystins, anatoxins, anatoxin-a, cylindrospermopsins, and saxitoxins [137].

Only in Figueira Gorda, both in October 2018 and February 2020, was a similar region of *mcy/nda*, responsible for producing Microcystin and Nodularin, detected. The *Cylindrospermopsis* gene cluster (*cyr*) was described from *Cylindrospermopsis*-producing genera, such as *Anabaena*, *Aphanizomenon* [138], and *Raphidiopsis curvata* F.E.Fritsch & M.F.Rich [139]. Two other genetic clusters were identified in *Cylindrospermopsis raciborskii* (Woloszynska) Seenayya & Subba Raju and included the polyketide synthetase (PKS) and non-ribosomal peptide synthetase (PPS). Although the function is still characterized as unclear, it is probably responsible for additional bioactive secondary metabolites synthesis [140]. *Cylindrospermopsis* is only produced when both genes are present in the DNA. The fact that only one of the genes was detected in Figueira Gorda in February 2020 means that the species present at that date were not producers of *Cylindrospermopsis*, perhaps because of intraspecific genetic variability. There is a probability that, due to climate change, the increasing temperature will contribute to the diffusion and success of *Cylindrospermopsis*-producing genera [141].

Water from reservoirs is often used for irrigation through illegal direct extractions, animal watering, and other domestic uses. Some authors point out that continuous exposure to contaminated water, even with low concentrations of cyanotoxins, may also pose a risk of chronic health effects [21,131,142]. Furthermore, there are risks associated with other routes of exposure, such as aerosols, during recreational activities, or from direct or indirect contact with contaminated water [142,143]. In addition, it has been documented that cyanotoxins can become accumulated in horticultural crops [144] with consequences for plant physiology and consumer health. Following [145], food safety is a major concern in most African countries due to the lack of knowledge, education, and sanitation, being a determinant to improve public health and nutrition security. Toxin accumulation patterns in edible fractions of plants and daily Microcystin–LR intake estimations that exceeded both the chronic reference dose (0.003 µg/kg of body weight) and total daily intake guidelines (0.04 µg/kg of body weight) in areas where eutrophic water sources were being used for irrigation were described by [146].

4.2.3. Relationship between Environmental Variables and Phytoplankton Descriptors

Phytoplankton productivity occurs under the influence of different abiotic variables, often interdependent and difficult to separate, which trigger the disorderly proliferation of species and bloom development [110,111,114]. In this sense, this study intends to determine, for the circumstances of the sampling, the influence or relationship between environmental variables and phytoplankton.

Nutrient availability has often been associated with higher primary productivity, which in situations of low N:P ratios promote the development of Cyanobacteria, since these organisms have the ability to fix N₂ [147,148], which was observed for 72% of all the analyzed samples. Consequently, P and N have been referred to as the main nutrients responsible for primary productivity [11,148]. Thus, the existence of negative correlations between phytoplankton metrics and nutrients could ensue from its assimilation and consequent transformation into biomass [148–151]. This was the case for the resulting negative models of chlorophytes and Cyanobacteria densities, with TN and NO₃-N in the first case and TP in the second case. The obtained models showed the importance of geology, with phytoplankton metrics dependent on micronutrient variables, which obviously do not determine primary productivity alone, but rather in association with other variables. Temperature is also a variable often associated with phytoplankton development, and particularly with cyanobacterial blooms [152]. In fact, the temperature was one of the independent variables in the model established for total biovolume, regardless of the low variation in air temperature (20.1–28.6 °C) recorded in the basins where reservoirs are located. This means that even with ideal temperature conditions throughout the year, the warmer months favor the development of phytoplankton. Likewise, precipitation, which tends to occur in warmer months, negatively influenced the model established for the density of Bacillariophyta. Therefore, these algae were present in a bloom situation

in the Saquinho reservoir in December 2017, which registered precipitation of around 2 mm. In this case, the reduced precipitation caused the environmental conditions for the proliferation of *Aulacoseira granulata* and *Cyclotella* sp., to the detriment of other algae.

5. Conclusions

The physicochemical results revealed that Santiago Island reservoirs only differ from each other in their geological influence variables. No separation by pressure variables was observed, which can be explained by the high concentrations of P and N recorded, above the Cape Verdean legislation and the limit for eutrophication. The high levels of P and N in water seem to be mainly due to LULC, which may be responsible for water quality degradation.

Considering the level of eutrophication registered during the study, the dominance of Cyanobacteria in the reservoirs with very high densities and biomass is not surprising. Thus, in all reservoirs, high-risk situations were identified, especially considering that the identified taxa are potential producers of different toxins. This is important for a region where the local population is supplied mostly from water sources not connected to the public network. The taxa responsible for this dominance were not the same in all reservoirs, emphasizing the role of local habitat factors on community composition and biodiversity (confirmation of the first hypothesis). The two β diversity indices emphasize complementary aspects in the temporal succession of taxa. Both indices highlight the wet period with more distinct assemblages, probably related to the higher concentrations of TP, which enter reservoirs from erosion processes caused by precipitation. The taxa variation/replacement among Santiago reservoirs seems to be the predominant mechanism in shaping phytoplankton γ diversity, and its biogeographic pattern reflects current environmental conditions, regardless of the geographic distance among systems.

In the studied reservoirs, phytoplankton productivity occurs under the influence of different abiotic variables, often interdependent and difficult to separate, which clarify the disorderly proliferation of species and bloom development. Chlorophyte and Cyanobacteria density showed negative correlations with nutrients, resulting from their assimilation and consequent transformation into biomass. Temperature and precipitation were also associated with phytoplankton development, which was observed for total biovolume and Bacillariophyta density, respectively (confirmation of the second hypothesis).

The present study provides useful information for Cyanobacteria bloom control and management strategies for reservoirs under semi-arid climate conditions, such as those in Santiago Island. Overall, the results reveal the importance of defining integrated management plans and strategies for the set of five reservoirs studied, since the processes influencing variation in the phytoplankton community are temporal-scale dependent, with similar biogeographic patterns. We encourage future studies, including large temporal-monitoring programs, to evaluate factors associated with shifts in cyanobacterial dominance to increase the level of confidence and safeguard human and animal health and the ecological integrity of the ecosystems. Therefore, understanding the relationship between LULC and reservoir services (Ecosystems Service consensus) is critical to improving ecosystem health and sustainability. For this, it is essential to involve local inhabitants and stakeholders to reach a consensus about LULC within reservoir drainage basins and surroundings in order to preserve ecosystems and promote the ecosystem services (e.g., irrigation and water supply).

Supplementary Materials: The following are available online at <https://www.mdpi.com/article/10.3390/w13202888/s1>, Table S1. Density (N° Cells/mL) of the phytoplankton taxa identified in each reservoir and sampling campaign. Table S2. Percentage breakdown of average dissimilarity among reservoirs, and sampling campaigns, using SIMPER analysis. Statistical and global R values for the pairwise analysis of similarity (ANOSIM) tests are presented, *** $p < 0.001$ and * $p < 0.05$ were considered significant. Table S3. Indicator taxa of the sampling months. Average abundance, average similarity, % of contribution and accumulative % are presented for the indicator taxa of each sampling month. Table S4. Cyanobacteria taxa, cell density (Cell/mL), and relative abundance of

each taxa identified in each reservoir (%). In bold, samples with relative abundance greater than 50%, are identified.

Author Contributions: Conceptualization, M.M., A.M.P. and M.H.N.; methodology, M.M., A.M.P., M.H.N. and L.L.; software, M.M., A.M.P., L.L. and S.S.V.; formal analysis, M.M., A.M.P., M.H.N., L.L. and S.S.V.; investigation, M.M., A.M.P., M.H.N., L.L. and S.S.V.; resources, M.M., L.L. and S.S.V.; writing—original draft preparation, M.M., A.M.P. and M.H.N.; writing—review and editing, M.M., A.M.P., M.H.N., L.L., S.S.V., E.A.M. and L.G.B. All authors have read and agreed to the published version of the manuscript.

Funding: This work was supported by national funding awarded by FCT-Foundation for Science and Technology, I.P., projects UIDB/04683/2020 and UIDP/04683/2020.

Institutional Review Board Statement: Not applicable.

Informed Consent Statement: Not applicable.

Acknowledgments: Authors thank the University of Cape Verde for the support given during the field campaigns in the five studied reservoirs; to Susana Nunes for the phytoplankton identification; and to Anabela Rosado and Inês Mavioso for the physicochemical analysis.

Conflicts of Interest: The authors declare no conflict of interest.

References

- Ramos, T.B.; Darouich, H.; Gonçalves, M.C.; Brito, D.; Castelo Branco, M.A.; Martins, J.C.; Fernandes, M.L.; Pires, F.P.; Morais, M.; Neves, R. An Integrated Analysis of the Eutrophication Process in the Enxoé Reservoir within the DPSIR. *Water* **2018**, *10*, 1576. [[CrossRef](#)]
- Palma, P.; Fialho, S.; Lima, A.; Mourinha, C.; Penha, A.; Novais, M.H.; Rosado, A.; Morais, M.; Potes, M.; Costa, M.J.; et al. Land-cover patterns and hydrogeomorphology of tributaries: Are these important stressors for the water quality of reservoirs in the Mediterranean region? *Water* **2020**, *12*, 2665. [[CrossRef](#)]
- Palma, P.; Penha, A.; Novais, M.H.; Fialho, S.; Lima, A.; Moutinho, C.; Alvarenga, P.; Rosado, A.; Iakunin, M.; Rofrigues, G.; et al. Water-sediment physicochemical dynamics in a large reservoir in the Mediterranean region under multiple stressors. *Water* **2021**, *13*, 707. [[CrossRef](#)]
- Yahyaee, A.R.; Moridi, A.; Sarang, A. A new optimized model to control eutrophication in multi-purpose reservoirs. *Int. J. Environ. Sci. Technol.* **2021**, *18*, 3357–3370. [[CrossRef](#)]
- Sabater-Liesa, L.; Ginebreda, A.; Barcelo, D. Shifts of environmental and phytoplankton variables in a regulated river: A spatial-driven analysis. *Sci. Total Environ.* **2018**, *642*, 968–978. [[CrossRef](#)]
- Mishra, P.; Garg, V.; Dutt, K. Seasonal dynamics of phytoplankton population and water quality in Bidoli reservoir. *Environ. Monit. Assess.* **2019**, *191*, 130. [[CrossRef](#)]
- Liu, C.; Sun, X.; Su, L.; Cai, J.; Zhang, L.; Guo, L. Assessment of phytoplankton community structure and water quality in the Hongmen Reservoir. *Water Qual. Res. J.* **2021**, *56*, 19–30. [[CrossRef](#)]
- Guedes, I.A.; Rachid, C.T.C.C.; Rangel, L.M.; Silva, L.H.S.; Bisch, P.M.; Azevedo, S.M.F.O.; Pacheco, A.B.F. Close link between harmful cyanobacterial dominance and associated bacterioplankton in a tropical eutrophic reservoir. *Front. Microbiol.* **2018**, *9*, 424. [[CrossRef](#)]
- Novais, M.H.; Penha, A.M.; Morales, E.A.; Potes, M.; Salgado, R.; Morais, M. Vertical distribution of benthic diatoms in a large reservoir (Alqueva, Southern Portugal) during thermal stratification. *Sci. Total Environ.* **2019**, *659*, 1242–1255. [[CrossRef](#)]
- Vanderley, R.F.; Ger, K.A.; Becker, V.; Bezerra, M.G.T.A.; Panosso, R. Abiotic factors driving cyanobacterial biomass and composition under perennial bloom conditions in tropical latitudes. *Hydrobiologia* **2021**, *848*, 943–960. [[CrossRef](#)]
- Guignard, M.S.; Leitch, A.R.; Acquisti, C.; Eizaguirre, C.; Elser, J.J.; Hessen, D.O.; Jeyasingh, P.D.; Neiman, M.; Richardson, A.E.; Soltis, P.S.; et al. Impacts of nitrogen and phosphorus: From genomes to natural ecosystems and agriculture. *Front. Ecol. Evol.* **2017**, *5*, 70. [[CrossRef](#)]
- Merel, S.; Villarín, M.C.; Chung, K.; Snyder, S. Spatial and thematic distribution of research on cyanotoxins. *Toxicon* **2013**, *76*, 118–131. [[CrossRef](#)]
- Merel, S.; Walker, D.; Chicana, R.; Snyder, S.; Baure's, E.; Thomas, O. State of knowledge and concerns on cyanobacterial blooms and cyanotoxins. *Environ. Int.* **2013**, *59*, 303–327. [[CrossRef](#)] [[PubMed](#)]
- Paerl, H.W. Mitigating toxic planktonic cyanobacterial blooms in aquatic ecosystems facing increasing anthropogenic and climatic pressures. *Toxins* **2018**, *10*, 76. [[CrossRef](#)] [[PubMed](#)]
- Paerl, H.W.; Huisman, J. Climate: Blooms like it hot. *Science* **2008**, *320*, 57–58. [[CrossRef](#)] [[PubMed](#)]
- Burford, M.A.; Beardall, J.; Willis, A.; Orr, P.T.; Magalhaes, V.F.; Rangel, L.M.; Azevedo, S.M.F.O.E.; Neilan, B.A. Understanding the winning strategies used by the bloom-forming cyanobacterium *Cylindrospermopsis raciborskii*. *Harmful Algae* **2016**, *54*, 44–53. [[CrossRef](#)]

17. Harke, M.J.; Davis, T.W.; Watson, S.B.; Gobler, C.J. Nutrient-controlled niche differentiation of western Lake Erie cyanobacterial populations revealed via metatranscriptomic surveys. *Environ. Sci. Technol.* **2016**, *50*, 604–615. [[CrossRef](#)]
18. Paerl, H.W. Controlling harmful cyanobacterial blooms in a climatically more extreme world: Management options and research needs. *J. Plankton Res.* **2017**, *39*, 763–771. [[CrossRef](#)]
19. Salmaso, N.; Boscaini, A.; Capelli, C.; Cerasino, L. Ongoing ecological shifts in a large lake are driven by climate change and eutrophication: Evidences from a three decade study in Lake Garda. *Hydrobiologia* **2018**, *824*, 177–195. [[CrossRef](#)]
20. Scherer, P.I.; Raeder, U.; Geist, J.; Zwirgmaier, K. Influence of temperature, mixing, and addition of microcystin-LR on microcystin gene expression in *Microcystis aeruginosa*. *Microbiology* **2017**, *6*, e00393. [[CrossRef](#)]
21. Buratti, M.F.; Manganelli, M.; Vichi, S.; Stefanelli, M.; Scardala, S.; Testai, E.; Funari, F. Cyanotoxins: Producing organisms, occurrence, toxicity, mechanism of action and human health toxicological risk evaluation. *Arch. Toxicol.* **2017**, *91*, 1049–1130. [[CrossRef](#)]
22. Carmichael, W.W.; Mahmood, N.A.; Hyde, E.G. Natural toxins from cyanobacteria (blue-green algae). In *Marine Toxins: Origins, Structure, and Molecular Pharmacology*; Hall, S., Strichartz, G., Eds.; American Chemical Society: Washington, DC, USA, 1990; pp. 87–106.
23. Christiansen, G.; Fastner, J.; Erhard, M.; Börner, T.; Dittmann, E. Microcystin biosynthesis in *Planktothrix*: Genes, evolution, and manipulation. *J. Bacteriol.* **2003**, *185*, 564–572. [[CrossRef](#)]
24. Rouhiainen, L.; Vakkilainen, T.; Siemer, B.L.; Buikema, W.; Haselkorn, R.; Sivonen, K. Genes coding for hepatotoxic heptapeptides (microcystins) in the cyanobacterium *Anabaena* strain 90. *Appl. Environ. Microbiol.* **2004**, *70*, 686–692. [[CrossRef](#)]
25. Moffitt, M.C.; Neilan, B.A. Characterization of the nodularin synthetase gene cluster and proposed theory of the evolution of cyanobacterial hepatotoxins. *Appl. Environ. Microbiol.* **2004**, *70*, 6353–6362. [[CrossRef](#)]
26. Stal, L.; Albertano, P.; Bergman, B.; von Brockel, K.; Gallon, J.; Hayes, P.; Sivonen, K.; Walsby, A. BASIC: Baltic Sea cyanobacteria. An investigation of the structure and dynamics of water blooms of cyanobacteria in the Baltic Sea—responses to a changing environment. *Cont. Shelf Res.* **2003**, *23*, 1695–1714. [[CrossRef](#)]
27. Lind, O.; Dávalos-Lind, L.; López, C.; López, M.; Dyble Bressie, J. Seasonal morphological variability in an in-situ Cyanobacteria monoculture: Example from a persistent *Cylindrospermopsis* bloom in Lake Catemaco, Veracruz, Mexico. *J. Limnol.* **2016**, *75*, 66–80. [[CrossRef](#)]
28. Figueredo, C.C.; Giani, A. Phytoplankton community in the tropical lake of Lagoa Santa (Brazil): Conditions favoring a persistent bloom of *Cylindrospermopsis raciborskii*. *Limnologia* **2009**, *39*, 264–272. [[CrossRef](#)]
29. Figueredo, C.C.; Pinto-Coelho, R.M.; Lopes, A.M.M.B.; Lima, P.H.O.; Gücker, B.; Giani, A. From intermittent to persistent cyanobacterial blooms: Identifying the main drivers in an urban tropical reservoir. *J. Limnol.* **2016**, *75*, 445–454. [[CrossRef](#)]
30. Giani, A.; Taranu, Z.E.; von Ruckert, G.; Gregory-Eaves, I. Comparing key drivers of cyanobacteria biomass in temperate and tropical systems. *Harmful Algae* **2017**, *97*, 101859. [[CrossRef](#)]
31. Medeiros, L.; Mattos, A.; Lürling, M.; Becker, V. Is the future blue-green or brown? The effects of extreme events on phytoplankton dynamics in a semi-arid man-made lake. *Aquat. Ecol.* **2015**, *49*, 293–307. [[CrossRef](#)]
32. Brasil, J.; Attayde, J.L.; Vasconcelos, F.R.; Dantas, D.D.F.; Huszar, V.L.M. Drought-induced water-level reduction favors cyanobacteria blooms in tropical shallow lakes. *Hydrobiologia* **2016**, *770*, 145–164. [[CrossRef](#)]
33. Costa, M.R.A.; Menezes, R.F.; Sarmiento, H.; Attayde, J.L.; da SL Sternberg, L.; Becker, V. Extreme drought favors potential mixotrophic organisms in tropical semiarid reservoirs. *Hydrobiologia* **2019**, *831*, 43–54. [[CrossRef](#)]
34. Tilahun, S.; Kifle, D. The influence of El Niño-induced drought on cyanobacterial community structure in a shallow tropical reservoir (Koka Reservoir, Ethiopia). *Aquat. Ecol.* **2019**, *53*, 61–77. [[CrossRef](#)]
35. Olds, B.P.; Peterson, B.C.; Koupal, K.D.; Farnsworth, K.M.; Schoenebeck, C.W.; Hoback, W.W. Water quality parameters of a Nebraska reservoir differ between drought and normal conditions. *Lake Reserv. Manag.* **2011**, *27*, 229–234. [[CrossRef](#)]
36. Mosley, L.M. Drought impacts on the water quality of freshwater systems; review and integration. *Earth-Sci. Rev.* **2015**, *140*, 203–214. [[CrossRef](#)]
37. McGregor, G.B.; Fabbro, L.D. Dominance of *Cylindrospermopsis raciborskii* (Nostocales, Cyanoprokaryota) in Queensland tropical and subtropical reservoirs: Implications for monitoring and management. *Lakes Reserv. Manag.* **2000**, *5*, 195–205. [[CrossRef](#)]
38. Crossetti, L.O.; de C. Bicudo, D.; Bini, L.M.; Dala-Corte, R.B.; Ferragut, C.; Bicudo, C.E.M. Plankton species interactions and invasion by *Ceratium furcoides* are influenced by extreme drought and water-hyacinth removal in a shallow tropical reservoir. *Hydrobiologia* **2019**, *831*, 71–85. [[CrossRef](#)]
39. Rotenberg, E.; Yakir, D. Contribution of semi-arid forests to the climate system. *Science* **2010**, *327*, 451–454. [[CrossRef](#)]
40. Huang, J.; Guan, X.; Ji, F. Enhanced cold-season warming in semi-arid regions. *Atmos. Chem. Phys.* **2012**, *12*, 5391–5398. [[CrossRef](#)]
41. Ventura, J.E. A problemática dos Recursos Hídricos em Santiago. In Proceedings of the 1º Congresso de Desenvolvimento Regional de Cabo Verde. 15º Congresso da ADPR | 2ª Congresso Lusófono de Ciência Regional | 3ª Congresso de Gestão e Conservação da Natureza, Cidade da Praia, Santiago, Cabo Verde, 6–11 July 2009.
42. Teixeira, J.J.L. Hidrosedimentologia e Disponibilidade Hídrica da Bacia Hidrográfica da Barragem de Poilão, Cabo Verde Análise de Riscos de Ruptura de Barragens: Estudo de Caso de Seis Barragens na Ilha de Santiago em Cabo Verde. Master's Thesis, Programa de Pós-Graduação em Engenharia Agrícola da Universidade Federal do Ceará, Fortaleza, Brazil, 2011; 100p.

43. Tavares dos Santos, E.A. As Barragens em Cabo Verde: Avaliação dos Impactes Ambientais, Socioeconómicos e Culturais. Caso de Estudo “A Barragem do Poilão” Ilha de Santiago. Master’s Thesis, em Gestão do Território—Especialização em Ambiente e Recursos Naturais, Universidade Nova de Lisboa, Lisboa, Portugal, 2013; 131p.
44. Lopes Varela, I.L.B. Estudo de Aproveitamento de fins Múltiplos da Barragem de Faveta, Ilha de Santiago (Cabo Verde) com Enfoque na rega e Abastecimento de Água. Master’s Thesis, Engenharia Civil na Especialidade de Hidráulica, Recursos Hídricos e Ambiente, Universidade de Coimbra, Coimbra, Portugal, 2014; 70p.
45. Araújo, A.; Hernandez, R.; Fonseca, R.; Matos, J. Avaliação da taxa de sedimentação na Barragem do Poilão (Ilha de Santiago, Cabo Verde). *Commun. Geológicas* **2014**, *10*, 597–600.
46. Ferreira, V.A.D.S. Conflitos e Participação no Uso da Água da Barragem de Poilão, Ilha de Santiago, Cabo Verde. Ph.D. Thesis, em Ciências Sociais, Universidade de Cabo Verde, Praia, Cabo Verde, 2014; 193p.
47. Instituto Nacional de Estatística (INE). *Inquérito Multi-Objetivo Contínuo (IMC)*; Instituto Nacional de Estatística (INE): Praia, Cabo Verde, 2019.
48. Gomes, A.D.M. Hidrogeologia e recursos hídricos da Ilha de Santiago (Cabo Verde). Ph.D. Thesis, Universidade de Aveiro, Aveiro, Portugal, 2007; 298p.
49. Bosa, M.S. Water Institutions and Management in Cape Verde. *Water* **2015**, *7*, 2641–2655. [[CrossRef](#)]
50. Marques, F.O.; Hildenbrand, A.; Zeyen, H.; Cunha, C.; Victória, S.S. The complex vertical motion of intraplate oceanic islands assessed in Santiago Island, Cape Verde. *Geochem. Geophys.* **2020**, *21*, e2019GC008754. [[CrossRef](#)]
51. Neves, D.J.D.; de P.R. Silva, V.; Almeida, R.S.R.; Sous, F.A.S.; da Silva, B.B. General aspects of the climate in the Cabo Verde archipelago. *Ambiência* **2017**, *13*, 59–73. [[CrossRef](#)]
52. Romeiras, M.M.; Duarte, M.C.; Pais, M.S. *Islands Biodiversity: Conservation Strategies Based on Knowledge of Endemic Plant Species from Cape Verde Islands [Macaronesian Region]*; Handbook of Nature Conservation: Global, Environmental and Economic Issues; Aronoff, J.B., Ed.; Nova Science Publishers, Inc.: New York, NY, USA, 2009; p. 147.
53. Correia de Matos, S.C. Padrões de Distribuição da Flora Exótica em Cabo Verde: O Papel dos Fatores Antrópicos e Ecológicos. Master’s Thesis, Ecologia e Gestão Ambiental, Universidade de Lisboa, Lisboa, Portugal, 2012; 53p.
54. Duarte, M.C.; Moreira, I. A vegetação de Santiago (Cabo Verde), Apontamento Histórico Garcia de Orta. *Ser. Bot.* **2002**, *16*, 51–80.
55. Fernandes, M.M. Análise de Risco de Ruptura de Barragens: Estudo de caso de seis Barragens na Ilha de Santiago em Cabo Verde, África. Ph.D. Thesis, Centro de Tecnologia, Engenharia Civil: Recursos Hídricos, Universidade Federal do Ceará, Fortaleza, Brazil, 2020; 381p.
56. Serralheiro, A. *Carta geológica da Ilha de Santiago (Cabo Verde) na Escala 1:100,000*. Junta de Investigações Científicas do Ultramar; Laboratório de Estudos Petrológicos e Paleontológicos do Ultramar: Lisboa, Portugal, 1977.
57. Instituto Nacional de Gestão do Território (INGT). Cabo Verde. 2018. Available online: <https://ingt.gov.cv/ingt/> (accessed on 24 May 2021).
58. Rice, E.W.; Baird, R.B.; Eaton, A.D.; Clesceri, L.S. (Eds.) *Standard Methods for the Examination of Water and Wastewater*, 22nd ed.; American Public Health Association (APHA); American Water Works Association (AWWA); Water Environmental Federation: Washington, DC, USA, 2012; ISBN 978-087553-013-0.
59. Cole, G.A. *Textbook of Limnology*, 4th ed.; Waveland Press Inc.: Long Grive, IL, USA, 1994.
60. INAG, I.P. *Manual para a Avaliação da Qualidade Biológica da água. Protocolo de Amostragem e Análise para o Fitoplâncton*; Ministério do Ambiente, do Ordenamento do Território e do Desenvolvimento Regional. Instituto da Água, I.P.: Lisboa, Portugal, 2009; 42p.
61. Huber-Pestalozzi, G. Das Phytoplankton des Süßwassers, Systematik und Biologie, 4. Teil: Euglenophyceen. *Die Binnengewässer* **1955**, *16*, 1–606.
62. Huber-Pestalozzi, G. *Das Phytoplankton des Süßwassers Band 16, 2 Teil, 1 Hälfte: Chrysophyceen. Farblose Flagellaten, Heterokonten*; Schweizerbart’sche Verlagsgesellschaft: Stuttgart, Germany, 1976.
63. Komárek, J.; Fott, B. *Chlorophyceae (Grünalgen), Ordnung Chlorococcales*. G. Huber-Pestalozzi, Ed. *Die Binnengewässer. Das Phytoplankton des Süßwassers, 7. Teil, 1. Hälfte*; E, Schweizerbart’sche Verlagsbuchhandlung: Stuttgart, Germany, 1983.
64. Komárek, J.; Komárková, J. Diversity of *Aphanizomenon*-like cyanobacteria. *Czech Phycol.* **2006**, *6*, 1–32.
65. Coesel, P.; Meesters, K. *Desmids of the Lowlands: Mesotaeniaceae and Desmidiaceae of the European Lowlands*; BRILL: Leiden, The Netherlands, 2007.
66. Coesel, P.; Meesters, K. *European Flora of the Desmid Genera Staurastrum and Staurodesmus: Identification Key for Desmidiaceae—Morphology—Ecology and Distribution—Taxonomy*; BRILL: Leiden, The Netherlands, 2013. [[CrossRef](#)]
67. McGregor, G.B. Freshwater Cyanobacteria of North-eastern Australia: 2: Chroococcales. *Phytotaxa* **2013**, *133*, 1–130. [[CrossRef](#)]
68. McGregor, G.B. Freshwater Cyanobacteria of North-Eastern Australia: 3. Nostocales. *Phytotaxa* **2018**, *359*, 1–166. [[CrossRef](#)]
69. Utermöhl, H. Zur Vervollkommnung der quantitativen Phytoplankton Methodik. *Int. Ver. Theor. Angew. Limnol.* **1958**, *9*, 1–38. [[CrossRef](#)]
70. Hillebrand, H.; Dürselen, C.-D.; Kirschtel, D.; Pollingher, U.; Zohary, T. Biovolume calculation for pelagic and benthic microalgae. *J. Phycol.* **1999**, *35*, 403–424. [[CrossRef](#)]
71. Sun, J.; Liu, D. Geometric models for calculating cell biovolume and surface area for phytoplankton. *J. Plankton Res.* **2003**, *25*, 1331–1346. [[CrossRef](#)]

72. INAG, I.P. *Manual para a Avaliação da Qualidade Biológica da água. Guia de Utilização da Tabela de Valores-Guia Normalizados de Biovolumes e Determinação do Biovolume Através de Procedimentos Laboratoriais*; Ministério da Agricultura, Mar, Ambiente e Ordenamento do Território. Instituto da Água, I.P.: Lisbon, Portugal, 2011; 11p.
73. Hammer, D.A.T.; Ryan, P.D.; Hammer, Ø.; Harper, D.A.T. Past: Paleontological Statistics Software Package for Education and Data Analysis. *Palaeontol. Electron.* **2001**, *4*, 1–9.
74. Shannon, C.; Weaver, W.W. *The Mathematical Theory of Communications*; University of Illinois Press: Champaign, IL, USA, 1963.
75. Death, R. Margalef's index. *Ecol. Indic.* **2008**, *2008*, 2209–22010.
76. Pielou, E.C. *Ecological Diversity*; John Wiley&Sons: New York, NY, USA, 1975; 174p.
77. Harrison, S.; Ross, S.J.; Lawton, J.H. Beta diversity on geographic gradients in Britain. *J. Anim. Ecol.* **1992**, *61*, 151–158. [[CrossRef](#)]
78. World Health Organization (WHO). Algae and cyanobacteria in fresh water. In *Guidelines for Safe Recreational Water Environments; Coastal and Fresh Waters*; World Health Organization: Geneva, Switzerland, 2003; Volume 1, pp. 136–158. Available online: <http://apps.who.int/iris/bitstream/10665/42591/1/9241545801.pdf> (accessed on 15 July 2021).
79. Videira, A. *Engenharia Genética—Princípios e Aplicações*; Lidel—edições técnicas. Lda: Lisbon, Portugal, 2011; ISBN 9789727577439.
80. Neiland, B.A.; Jacobs, D.; Del Dot, T.; Blackall, L.L.; Hawkings, P.R.; Cox, P.T.; Goodman, C.A. rRNA sequences and evolutionary relationships among toxic and nontoxic cyanobacteria of the genus *Microcystis*. *Int. J. Syst. Bacteriol.* **1997**, *47*, 693–697. [[CrossRef](#)]
81. Jungblut, A.D.; Hawes, I.; Mountfort, D.; Hitzfeld, B.; Dietrich, D.R.; Burns, B.P.; Neilan, B.A. Diversity within cyanobacterial mat communities in variable salinity meltwater ponds of McMurdo Ice Shelf, Antarctica. *Environ. Microbiol.* **2005**, *7*, 519–529. [[CrossRef](#)]
82. Nonnemam, D.; Zimba, P.V. A PCR-based test to assess the potential for microcystins occurrence in channel catfish production ponds. *J. Phycol.* **2002**, *38*, 230–233. [[CrossRef](#)]
83. Jungblut, A.-D.; Neilan, B.A. Molecular identification and evolution of the cyclic peptide hepatotoxins, microcystins, and nodularins synthetase genes in three orders of Cyanobacteria. *Arch. Microbiol.* **2006**, *186*, 107–114.
84. Schembri, M.A.; Neilan, B.A.; Saint, C.P. *Identification of Genes Implicated in Toxins Production in the *Cylindrospermopsis Raciborskii**; John Wiley & Sons, Inc.: New York, NY, USA, 2001; pp. 413–421.
85. Singh, K.P.; Malik, A.; Mohan, D.; Sinha, S. Multivariate statistical techniques for the evaluation of spatial and temporal variations in water quality of Gomti River (India)—A case study. *Water Res.* **2004**, *38*, 3980–3992. [[CrossRef](#)]
86. Clarke, K.; Gorley, R. Non-parametric multivariate analyses of changes in community structure. *Aust. J. Ecol.* **1993**, *18*, 117–143. [[CrossRef](#)]
87. Clarke, K.; Gorley, R. *Primer E-v5: User Manual/Tutorial. Primer-E, Plymouth*; Plymouth Marine Laboratory: Plymouth, UK, 2001.
88. Victória, S.S. *Caraterização Geológica e Geotécnica das Unidades Litológicas da Cidade da Praia (Santiago, Cabo Verde)*. Ph.D. Thesis, DCT-FCT, Universidade de Coimbra, Coimbra, Portugal, 2012; 302p.
89. Serralheiro, A. *A Geologia da ilha de Santiago (Cabo Verde)*. Ph.D. Thesis, Museu do Laboratório Mineralógico e Geológico da Faculdade de Ciências da Universidade de Lisboa, Universidade de Lisboa, Lisboa, Portugal, 1976; 218p.
90. da, S.C. Pinto, M.M. *Cartografia Geoquímica da ilha de Santiago com uma DENSIDADE de Amostragem Média/Baixa (Geochemical Mapping of Santiago Island with a Medium/Low Sampling Density)*. Ph.D. Thesis, Geoscience, University of Aveiro, Aveiro, Portugal, 2010; 436p.
91. Vanni, M.J. Nutrient cycling by animals in freshwater ecosystems. *Annu. Rev. Ecol. Syst.* **2002**, *33*, 341–370. [[CrossRef](#)]
92. Schmidt, T.S.; Clements, W.H.; Wanty, R.B.; Verplanck, P.L.; Church, S.E.; San Juan, C.A.; Fey, D.L.; Rockwell, B.W.; Dewitt, E.D.H.; Klein, T.L. Geologic processes influence the effects of mining on aquatic ecosystems. *Ecol. Appl.* **2012**, *22*, 870–879. [[CrossRef](#)] [[PubMed](#)]
93. Bouwman, A.F.; Bierkens, M.F.P.; Griffioen, J.; Hefting, M.M.; Middelburg, J.; Middelkoop, H.; Slomp, C.P. Nutrient dynamics, transfer and retention along the aquatic continuum from land to ocean: Towards integration of ecological and biogeochemical models. *Biogeosciences* **2013**, *10*, 1–23. [[CrossRef](#)]
94. Lintern, A.; Webb, J.A.; Ryu, D.; Liu, S.; Bende-Michl, U.; Waters, D.; Leahy, P.; Wilson, P.; Western, A.W. Key factors influencing differences in stream water quality across space. *WIREs Water* **2018**, *5*, e1260. [[CrossRef](#)]
95. Dubois, N.; Saulnier-Talbot, E.; Mills, K.; Gell, P.; Battarbee, R.; Bennion, H.; Chawchai, S.; Dong, X.; Francus, P.; Flower, R.; et al. First human impacts and responses of aquatic systems: A review of palaeolimnological records from around the world. *Anthr. Rev.* **2018**, *5*, 28–68. [[CrossRef](#)]
96. Strayer, D.L.; Beighley, R.E.; Thompson, L.C.; Brooks, S.; Nilsson, C.; Pinay, G.; Naiman, R.J. Effects of land-cover change on stream ecosystems: Roles of empirical models and scaling issues. *Ecosystems* **2003**, *6*, 407–423. [[CrossRef](#)]
97. Zhang, D.; Wang, X.; Zhou, Z. Impacts of small-scale industrialized swine farming on local soil, water and crop qualities in a hilly red soil region of subtropical China. *Int. J. Environ. Res. Public Health* **2017**, *14*, 1524. [[CrossRef](#)]
98. Zhou, Y.; Xu, J.F.; Yin, W.; Ai, L.; Fang, N.F.; Tan, W.F.; Yan, F.L.; Shi, Z.H. Hydrological and environmental controls of the stream nitrate concentration and flux in a small agricultural watershed. *J. Hydrol.* **2017**, *545*, 355–366. [[CrossRef](#)]
99. Matono, P.; Batista, T.; Sampaio, E.; Ilhéu, M. Effects of Agricultural Land Use on the Ecohydrology of Small-Medium Mediterranean River Basins: Insights from a Case Study in the South of Portugal. In *Land Use—Assessing the Past, Envisioning the Future*; InTechOpen: London, UK, 2018; pp. 30–51.
100. Messina, N.J.; Couture, R.M.; Norton, S.A.; Birkel, S.D.; Amirbahman, A. Modeling response of water quality parameters to land-use and climate change in a temperate, mesotrophic lake. *Sci. Total Environ.* **2010**, *713*, 136549. [[CrossRef](#)]

101. Vásquez-Méndez, R.; Ventura-Ramos, E.; Oleschko, K.; Hernández-Sandoval, L.; Angel Domínguez-Cortázar, M. *Soil Erosion Processes in Semiarid Areas: The Importance of Native Vegetation, Soil Erosion Studies*; InTech: London, UK, 2011; pp. 25–40, ISBN 978-953-307-710-9. Available online: <File:///C:/Users/Manuela%20Morais/Downloads/IntechsoilerosionISBN978-953-307-435-1.pdf> (accessed on 15 July 2021).
102. Scholes, R.J. The Future of Semi-Arid Regions: A Weak Fabric Unravels. *Climate* **2020**, *8*, 43. [[CrossRef](#)]
103. Bou-Imajjane, L.; Belfoul, M.A.; Elkadiri, R.; Stokes, M. Soil erosion assessment in a semi-arid environment: A case study from the Argana Corridor, Morocco. *Environ. Earth Sci.* **2020**, *79*, 409. [[CrossRef](#)]
104. FitzHugh, T.W.; Mackay, D.S. Impact of subwatershed partitioning on model source-and transport-limited sediment yields in an agricultural nonpoint source pollution model. *J. Soil Water Conserv.* **2001**, *56*, 137–143.
105. Thurow, T.L.; Taylor, C.H., Jr. Viewpoint: The role of drought in range management. *J. Range Manag.* **1999**, *52*, 413–419. [[CrossRef](#)]
106. Nunes, J.P.; Seixas, J.; Keizer, J.J. Modeling the response of within-storm runoff and erosion dynamics to climate change in two Mediterranean watersheds: A multi-model, multi-scale approach to scenario design and analysis. *Catena* **2013**, *102*, 27–39. [[CrossRef](#)]
107. Lisboa, M.S.; Schneider, R.L.; Sullivan, P.J.; Walter, M.T. Drought and post-drought rain effect on stream phosphorus and other nutrient losses in the Northeastern USA. *J. Hydrol. Reg. Stud.* **2020**, *28*, 100672. [[CrossRef](#)]
108. Green, R.; Bertetti, F.; Hernandez, M. Recharge Variability in Semi-Arid Climates. *Nat. Educ. Knowl.* **2012**, *3*, 34.
109. Smith, V.H. Eutrophication of freshwater and coastal marine ecosystems a global problem. *Environ. Sci. Pollut. Res.* **2003**, *10*, 126–139. [[CrossRef](#)] [[PubMed](#)]
110. Baho, D.L.; Drakare, S.; Johnson, R.K.; Allen, C.R.; Angeler, D.G. Is the impact of eutrophication on phytoplankton diversity dependent on lake volume/ecosystem size? *J. Limnol.* **2017**, *76*, 199–210.
111. Huisman, J.; Codd, G.A.; Paerl, H.W.; Ibelings, B.W.; Verspagen, J.M.H.; Visser, P.M. Cyanobacterial blooms. *Nat. Rev. Microbiol.* **2018**, *16*, 471–483. [[CrossRef](#)]
112. Burford, M.A.; O'Donohue, M.J. A comparison of phytoplankton community assemblages in artificially and naturally mixed subtropical water reservoirs. *Freshw. Biol.* **2006**, *51*, 973–982. [[CrossRef](#)]
113. Istvánovics, V. Eutrophication of Lakes and Reservoirs. In *Encyclopedia of Inland Waters*; Likens, G.E., Ed.; Elsevier: Oxford, UK, 2009; Volume 1, pp. 157–165.
114. Vinçon-Leite, B.; Casenave, C. Modelling eutrophication in lake ecosystems: A review. *Sci. Total Environ.* **2019**, *651*, 2985–3001. [[CrossRef](#)]
115. Leibold, M.A.; Holyoak, M.; Mouquet, N.; Amarasekare, P.; Chase, J.M.; Hoopes, M.F.; Holt, R.D.; Shurin, R.B.; Law, R.; Tilman, D.; et al. The metacommunity concept: A framework for multi-scale community ecology. *Ecol. Lett.* **2004**, *7*, 601–613. [[CrossRef](#)]
116. Holyoak, M.; Leibold, M.A.; Holt, R.D. *Metacommunities: Spatial Dynamics and Ecological Communities*; The University of Chicago Press: Chicago, IL, USA, 2005.
117. Elliott, J.A.; Persson, I.; Thackeray, S.J.; Blenckner, T. Phytoplankton modelling of Lake Erken, Sweden by linking the models PROBE and PROTECH. *Ecol. Modell.* **2007**, *202*, 421–426. [[CrossRef](#)]
118. Soininen, J. A quantitative analysis of species sorting across organisms and ecosystems. *Ecology* **2014**, *95*, 3284–3292. [[CrossRef](#)]
119. Bond, N.R.; Lake, P.S.; Arthington, A.H. The impacts of drought on freshwater ecosystems: An Australian perspective. *Hydrobiologia* **2008**, *600*, 3–16. [[CrossRef](#)]
120. Zorzal-Almeida, S.; Bartzek, E.C.R.; Bicudo, D.C. Homegenization of diatom assemblages is driven by eutrophication in tropical reservoirs. *Environ. Pollut.* **2021**, *288*, 117778. [[CrossRef](#)] [[PubMed](#)]
121. Baselga, A. Partitioning the turnover and nestedness components of beta diversity. *Glob. Ecol. Biogeogr.* **2010**, *19*, 134–143. [[CrossRef](#)]
122. Rodríguez-Alcalá, O.; Blanco, S.; García-Girón, J.; Jeppesen, E.; Irvine, K.; Nöges, P.; Nöges, T.; Gross, E.M.; Bécares, E. Large-scale geographical and environmental drivers of shallow lake diatom metacommunities across Europe. *Sci. Total Environ.* **2020**, *707*, 135887. [[CrossRef](#)] [[PubMed](#)]
123. Whittaker, R.J.; Willis, K.J.; Field, R. Scale and species richness: Towards a general, hierarchical theory of species diversity. *J. Biogeogr.* **2001**, *28*, 453–470. [[CrossRef](#)]
124. Crispino, L.M.B.; Sant'Anna, C.L. Cianobactérias marinhas bentônicas de ilhas costeiras do Estado de São Paulo, Brasil. *Rer. Bras. Bot.* **2006**, *29*, 639–656. [[CrossRef](#)]
125. Tucci, A.; Sant'Anna, C.L.; Gentil, R.C.; Azevedo, M.T. daP. Fitoplâncton do Lago das Garças, São Paulo, Brasil: Um reservatório urbano eutrófico. *Hoehnea* **2006**, *33*, 147–175.
126. Havens, K.E.; Thomas, J.R.; East, T.L.; Smilth, V.H. N:P ratios, light limitation, and cyanobacterial dominance in a subtropical lake impacted by non-point source nutrient pollution. *Environ. Pollut.* **2003**, *122*, 379–390. [[CrossRef](#)]
127. Moresco, G.A.; Bortolini, J.C.; De'o Dias, J.; Pineda, A.; Jati, S.; Rodrigues, L.C. Drivers of phytoplankton richness and diversity components in Neotropical floodplain lakes, from small to large spatial scales. *Hydrobiologia* **2017**, *799*, 203–215. [[CrossRef](#)]
128. Finlay, B.J. Global dispersal of free-living microbial eukaryote species. *Science* **2002**, *296*, 1061–1063. [[CrossRef](#)]
129. Fenchel, T.; Finlay, B.J. The ubiquity of small species: Patterns of local and global diversity. *BioScience* **2004**, *54*, 777–784. [[CrossRef](#)]
130. Martiny, J.B.H.; Bohannan, B.J.M.; Brown, J.H.; Colwell, R.K.; Fuhrman, J.A.; Green, J.L.; Horner-Devine, M.C.; Kane, M.; Krums, J.A.; Kuske, C.R.; et al. Microbial biogeography: Putting microorganisms on the map. *Nat. Rev. Microbiol.* **2006**, *4*, 102–112. [[CrossRef](#)]

131. Funari, E.; Testai, E. Human health risk assessment related to cyanotoxins exposure. *Crit. Rev. Toxicol.* **2008**, *38*, 97–125. [[CrossRef](#)] [[PubMed](#)]
132. Whitton, B.A. *Ecology of Cyanobacteria II. Their Diversity in Space and Time*; Springer: New York, NY, USA, 2008; p. 760.
133. Rastogi, R.P.; Sinha, R.P.; Incharoensakdi, A. The cyanotoxin microcystins: Current overview. *Rev. Environ. Sci. Bio.* **2014**, *13*, 215–249. [[CrossRef](#)]
134. Corbel, S.; Mougín, C.; Bouaïcha, N. Cyanobacterial toxins: Modes of actions, fate in aquatic and soil ecosystems, phytotoxicity and bioaccumulation in agricultural crops. *Chemosphere* **2014**, *96*, 1–15. [[CrossRef](#)] [[PubMed](#)]
135. Niamien-Ebrotte, J.E.; Bhattacharyya, S.; Deep, P.R.; Nayak, B. Cyanobacteria and cyanotoxins in the world: Review. *Inter. J. App. Res.* **2015**, *1*, 563–569.
136. Mowe, M.; Mitrovic, S.; Lim, R.; Furey, A.; Yeo, D. Tropical cyanobacterial blooms: A review of prevalence, problem taxa, toxins and influencing environmental factors. *J. Limnol.* **2015**, *74*, 205–224. [[CrossRef](#)]
137. Chorus, I.; Welker, M. (Eds.) *Toxic Cyanobacteria in Water*, 2nd ed.; CRC Press: Boca Raton, FL, USA; World Health Organization: Geneva, Switzerland, 2021.
138. Stuken, A.; Campbell, R.J.; Quesada, A.; Sukenik, A.; Dadheech, P.K.; Wiedner, C. Genetic and morphologic characterization of four putative cylindrospermopsin producing species of the cyanobacterial genera Anabaena and Planktothrix. *J. Plankton Res.* **2009**, *31*, 465–480. [[CrossRef](#)]
139. Jiang, Y.; Xiao, P.; Yu, G.; Sano, T.; Pan, Q.; Li, R. Molecular basis and phylogenetic implications for deoxy-cylindrospermopsin biosynthesis in *Raphidiopsis curvata* (cyanobacteria). *Appl. Environ. Microbiol.* **2012**, *78*, 2256–2263. [[CrossRef](#)] [[PubMed](#)]
140. Sinha, R.; Pearson, L.A.; Davis, T.W.; Muenchhoff, J.; Pratama, R.; Jex, A.; Burford, M.A.; Neilan, B.A. Comparative genomics of *Cylindrospermopsis raciborskii* strains with differential toxicities. *BMC Genome.* **2014**, *15*, 83. [[CrossRef](#)]
141. Funari, E.; Manganelli, M.; Sinisi, L. Impact of climate change on waterborne diseases. *Ann. Ist. Super Sanità.* **2012**, *48*, 473–487. [[CrossRef](#)]
142. Zanchett, G.; Oliveira-Filho, E.C. Cyanobacteria and Cyanotoxins: From Impacts on Aquatic Ecosystems and Human Health to Anticarcinogenic Effects. *Toxins* **2013**, *5*, 1896–1917. [[CrossRef](#)] [[PubMed](#)]
143. Backer, L.C.; McNeel, S.; Barber, T.; Kirkpatrick, B.; Williams, C.; Irvin, M.; Zhou, Y.; Johnson, T.; Nierenberg, K.; Aubel, M.; et al. Recreation exposure to microcystins during an algal bloom in California lakes. *Toxins* **2010**, *55*, 909–921.
144. Gutiérrez-Praena, D.; Campos, A.; Azevedo, J.; Neves, J.; Freitas, M.; Guzmán-Guillén, R.; Cameán, A.M.; Renaut, J.; Vasconcelos, V. Exposure of *Lycopersicon esculentum* to Microcystin-LR: Effects in the Leaf Proteome and Toxin Translocation from Water to Leaves and Fruits. *Toxins* **2014**, *6*, 1837–1854. [[CrossRef](#)]
145. Ferrão, J.; Bell, V.; Fernandes, T.H. Mycotoxins, Food Safety and Security in Sub-Saharan Africa. *SM J. Food Nutri. Disord.* **2017**, *3*, 1021.
146. Lee, S.; Jiangb, X.; Manuboluc, M.; Riedlb, K.; Ludcina, S.A.; Martina, J.F.; Lee, J. Fresh produce and their soils accumulate cyanotoxins from irrigation water: Implications for public health and food security. *Food Res. Int.* **2017**, *102*, 234–245. [[CrossRef](#)]
147. Codd, G.A.; Steffensen, D.A.; Burch, M.D.; Baker, P.D. Toxic blooms of cyanobacteria in Lake Alexandrina: Learning from history. *Aust. J. Mar. Freshw. Res.* **1994**, *45*, 731–736. [[CrossRef](#)]
148. Lv, J.; Wu, H.; Chen, M. Effects of nitrogen and phosphorus on phytoplankton composition and biomass in 15 subtropical, urban shallow lakes in Wuhan, China. *Limnologia* **2011**, *41*, 48–56. [[CrossRef](#)]
149. Ahmed, A.I.; Mohamed, H.A.-A.; Takajio, O.; Nitrogen Fixing Cyanobacteria: Future Prospect. Open Access Peer-Reviewed Chapter. 2014. Available online: <https://www.intechopen.com/books/advances-in-biology-and-ecology-of-nitrogen-fixation/nitrogen-fixing-cyanobacteria-future-prospect> (accessed on 15 July 2021).
150. Li, Y.; Liu, Y.; Zhao, L.; Hastings, A.; Guo, H. Exploring change of internal nutrients cycling in a shallow lake: A dynamic nutrient driven phytoplankton model. *Ecol. Model.* **2015**, *313*, 137–148. [[CrossRef](#)]
151. Cui, Y.; Zhu, G.; Li, H.; Luo, L.; Cheng, X.; Jin, Y.; Trolle, D. Modelling the response of phytoplankton to reduced external nutrient load in a subtropical Chinese reservoir using DYRESM-CAEDYM. *Lake Reserv. Manag.* **2016**, *32*, 146–157. [[CrossRef](#)]
152. Elliott, J.A.; Defew, L. Modelling the response of phytoplankton in a shallow lake (Loch Leven, UK) to changes in lake retention time and water temperature. *Hydrobiologia* **2012**, *681*, 105–116. [[CrossRef](#)]